drones

MDPI

Article

EMI Analysis and Nonlinearity Characterization of 5G FR1 Amplifiers for UAV–RIS Networks

Muhammad Bilal Yaseen [1,2], Fayu Wan [1,*], Md Owahedur Rahman [1] and Fareeha Siddique [3]

[1] School of Electronics and Information Engineering, Nanjing University of Information Science & Technology (NUIST), Nanjing 210044, China; bilal@nuist.edu.cn (M.B.Y.); 202351180002@nuist.edu.cn (M.O.R.)
[2] Computer Science Department, Faculty of Computer Sciences, ILMA University, Karachi 75190, Pakistan
[3] School of Remote Sensing and Geomatics Engineering, Nanjing University of Information Science & Technology (NUIST), Nanjing 210044, China; fareeha@nuist.edu.cn
* Correspondence: fayu.wan@nuist.edu.cn

Abstract: This work introduces a broad framework for the enhanced nonlinearity assessment of PAs for 5G FR1 in UAV–RIS networks with integration. This study employs LabVIEW-based double-frequency IMD3 testing methodology for a fast automatic test bed to quantify the nonlinearity and its EMI effect on the UAV–RIS system. The analysis includes the evaluation of the EMI effect on the TxRx link using the SNR model. In order to enhance the efficiency of the system, a 16 QAM modulator is incorporated into the system in order to modulate and demodulate the signal. Additionally, the system includes a Deep Q agent based on the DRL model that enhances the controllability and efficiency of amplifiers under the dynamic environment typical for UAV–RIS networks. This work offers a framework for enhancing amplifier design for EMI reduction and supports the sound engineering of future UAV–RIS-based communication networks. The outcomes prove that signal integrity and nonlinearity characterization are enhanced significantly, providing important information for future 5G and beyond wireless communication systems.

Keywords: 5G FR1; GaN power amplifiers; electromagnetic interference; UAV–RIS; double-frequency testing

check for updates

Academic Editor: Carlos Tavares Calafate

Received: 24 February 2025
Revised: 9 April 2025
Accepted: 18 April 2025
Published: 24 April 2025

Citation: Yaseen, M.B.; Wan, F.; Rahman, M.O.; Siddique, F. EMI Analysis and Nonlinearity Characterization of 5G FR1 Amplifiers for UAV–RIS Networks. *Drones* **2025**, *9*, 328. https://doi.org/10.3390/drones9050328

Copyright: © 2025 by the authors. Licensee MDPI, Basel, Switzerland. This article is an open access article distributed under the terms and conditions of the Creative Commons Attribution (CC BY) license (https://creativecommons.org/licenses/by/4.0/).

1. Introduction

The emergence of 5G technology marks a revolutionary advancement in wireless communication, offering unprecedented data rates, ultra-low latency, and enhanced network reliability [1–5]. These features are instrumental in addressing the increasing demands for high-speed and efficient communication in various applications, from smart cities and autonomous vehicles to industrial automation and telemedicine [6–10]. However, to fully exploit the capabilities of 5G, innovative solutions are required to overcome the limitations of conventional communication infrastructure, particularly in scenarios with dynamic or challenging propagation environments [11–15]. One promising solution involves the integration of unmanned aerial vehicles (UAVs) with reconfigurable intelligent surfaces (RISs) [16–21]. UAVs have gained attention for their mobility, flexible deployment, and altitude control capabilities [22–25]. Such characteristics make UAVs suitable for delivering connectivity where needed, for instance, after disasters, during events requiring temporary networks, and in areas with no or weak physical infrastructure [26–29]. On the other hand, RIS technology brings a new concept in wireless communication, where surfaces actively control electromagnetic waves. Unlike conventional passive structures,

RISs can actively switch between reflection, refraction, or transmission of the incident waves and hence actively manipulate the wireless propagation channel to improve signal quality [30]. Integrating UAVs with RIS technology combines UAVs' mobility and deployment flexibility with RISs' ability to control the environment dynamically. [31–33]. This integration is believed to revolutionize wireless communication networks by offering better signal coverage, higher spectral efficiency, and lower interference [34]. For instance, the UAV-mounted RIS can alter its physical location and reflectivity patterns in real time to enhance the communication link between a transmitter and a receiver, especially in industrial zones [35–37].

These results highlight the importance of designing more sophisticated interference cancellation techniques, especially when multiple UAVs and RIS panels are in operation at the same time. Like Wu et al. [14], we also studied a self-interference cancellation technique for an RIS-based full-duplex communication system, but their work mainly focused on interference inside the transceiver, and they did not consider interference from the environment, especially when UAV mobility is involved.

Adam et al. [1] proposed an intelligent multiuser RIS communication method to address the difficulties of jittering UAVs and the limitation of imperfect hardware. Their well-built design uses adaptive beamforming to mitigate the impacts of UAV movement; however, the study noted that it is challenging to address nonlinearity from the PAs in the 5G FR1 band. This issue of PA nonlinearity has been a recurring problem, as pointed out by Khennoufa et al. [10], who presented an error performance analysis for UAV-mounted RIS in non-orthogonal multiple access (NOMA) systems. Their work also demonstrated that PAs exhibit nonlinear behavior, which results in high intermodulation distortion, hence the need for sophisticated methods of nonlinearity compensation. Abualhayja [2] targeted the model of beamforming strategies in RIS-assisted UAV communication systems. Some of the issues concerning dynamic channel conditions were considered in the study, in which new algorithms for trajectory construction and beam pointing were suggested. However, the model techniques presented here depend on the predetermined channel models, which may not be efficient in the dynamic environment common with UAV operations.

However, Weng and Chen [26] discussed the security issues in the multi-UAV networks and the need for dynamic solutions for RIS deployment. In [13], Sun et al. studied the application of RIS in integrated satellite-UAV networks and investigated the influence of co-channel interference and hardware distortion. Their work also pointed out that there is a need to develop better interference mitigation techniques that take into account both the RIS impairments and the mobility of the UAVs. Likewise, Yao et al. [33] investigated the UAV trajectory model in RIS-assisted air-to-ground communication networks, where energy-efficient algorithms are developed to minimize power consumption while maximizing communication quality. However, their methods do not fully address the challenges posed by power amplifier nonlinearity, which is a gap that has not been addressed in the current literature. Deep learning and reinforcement learning techniques have been suggested to be used as the solution to the problems in RIS-assisted UAV systems. Zou et al. [7] proposed a deep reinforcement learning solution for reliable beamforming in UAV communication with better performance in anti-jamming and eavesdropping environments. This is in line with the direction of our research, which focuses on using deep learning models for the adaptive control of RIS configurations and power amplifier settings. Likewise, You et al. [18] utilized deep reinforcement learning to enhance D2D communication in RIS-aided UAV networks, but they did not consider the dynamic nature of UAVs and the environment.

1.1. Background

The communication networks facilitated by UAV–RIS depend on GaN PAs to boost the output power of the transmitted signals for long-range transmission. In these networks, the nonlinearity of PAs can cause high levels of IMD, which in turn generate unwanted harmonics and spectral regrowth that cause EMI [1,26]. This interference can distort the quality of the transmitted signals and thus increase the bit error rate (BER) of the system. EMI effects worsen in dynamic environments, such as those involving UAVs, where channel and signal characteristics frequently fluctuate [13,25]. Furthermore, in UAV networks, reconfigurable intelligent surfaces (RISs) are used to control the electromagnetic wave to increase the signal range and reduce interference [9]. Nevertheless, the non-idealities in PAs and hardware impairments can degrade the ability of RISs in EMI reduction and hence reduce system performance [10,30]. This necessitates a framework to assess and categorize PA nonlinearity and its EMI impacts in UAV–RIS systems. Despite the progress made in the last few years in the development of RIS and UAV integration for improving wireless communications, some key issues remain unaddressed. The literature lacks studies that address the implementation issues of power amplifier nonlinearity and the dynamic nature of EMI in UAV–RIS systems. Furthermore, most of the existing research employs fixed or approximate channel and hardware models that cannot effectively mimic the real-world dynamic channel and hardware environment. This research intends to fill these gaps through the proposed comprehensive framework that entails real-time nonlinearity characterization and adaptive EMI mitigation through deep reinforcement learning. Through the identification of these unsolved questions, our work aims to improve the reliability and performance of future UAV–RIS-based communication systems.

However, the application of UAV–RIS systems, as discussed above, is not without some major technical concerns. These challenges stem from the complex interactivity between the high-frequency operations characteristic of the 5G FR1 band, the nonlinearity of power amplifiers (PAs), and the mobility of UAVs. Among the main concerns, the first one is related to the nonlinearity of PAs, which are typically operated at back-off points to achieve sufficient transmission range and signal power. This high-power operation causes a substantial amount of nonlinear behavior, which appears in the form of harmonics and intermodulation products, particularly third-order intermodulation distortion (IMD3). IMD3 is the most significant since it results in spectral regrowth, which interferes with other channels and degrades the quality of the transmitted signal [1,9]. Overcoming this nonlinearity is crucial to reduce distortion and guarantee the quality of message transmission in UAV–RIS systems. Another critical problem is electromagnetic interference (EMI) [37].

The incorporation of UAVs with RIS presents new electromagnetic coupling issues that can lead to critical EMI issues. As in most UAV–RIS scenarios, the signals reflected by the RIS can either combine constructively or destructively with the direct signals from the transmitter. This interference is further complicated by the fact that UAVs are highly mobile, and hence the propagation paths change very quickly, leading to interference patterns that also change very frequently [7,14]. Hence, effective EMI countermeasures are crucial in ensuring signal clarity and suppressing signal interferences in such mobile situations. The constantly varying and highly dynamic nature of the channel is another major challenge that UAV–RIS systems will face. Due to the mobility and altitude differences of UAVs, the CSI needs to be updated more frequently to match the current situation. This requires dynamic control of the RIS configuration to ensure that reflection properties are optimized and signal quality is high. Without such adaptability, the system fails to send out clear signals, and the performance of the network significantly decreases, limiting its functionality [32,35].

Furthermore, the efficiency of RISs in increasing the signal transmission range is highly sensitive to the accuracy of the reflective parts.

In practice, RIS panels are subjected to hardware limitations such as phase noise, inaccurate reflection coefficients, and synchronization with the UAV-mounted transceivers. These impairments can greatly reduce the ability of RISs to steer the signal beam and thus reduce the expected gains in signal strength and coverage [27,31]. Last but not least, energy efficiency and power limitation are critical issues in UAV–RIS systems due to the limited energy supply of UAVs. The energy consumption of UAVs is directly affected by the power consumption in the communication system and the power amplifiers. Higher-power operations required to compensate for path loss and provide good signal strength increase energy consumption and shorten UAV operation time [6,29]. Hence, achieving a trade-off between power consumption and the quality of the signal is a major concern in the design of energy-efficient UAV–RIS systems; it is crucial to develop new approaches that can increase the UAV's working time while maintaining high communication quality.

1.2. Problem Statement

The integration of UAVs with RIS has gained interest for enhancing 5G coverage and capacity but overlooks real-world challenges like PA nonlinearity and EMI, particularly in the 5G FR1 band. Current solutions fail to address the dynamic nature of UAV–RIS systems and lack adaptive control mechanisms.

The introduction of UAV–RIS to reconfigurable intelligent surfaces (RISs) in 5G addresses key challenges that traditional static RISs cannot solve, particularly in highly dynamic and obstructed environments. While the conventional RIS improves signal propagation by passive beamforming, its fixed position limits adaptability in scenarios where users are mobile or obstacles frequently change (e.g., urban canyons, disaster recovery zones). UAV–RIS overcomes this by providing real-time repositioning, ensuring optimal signal reflection and extending coverage to non-line-of-sight (NLOS) users, which is crucial for beyond-5G (B5G) ultra-reliable low-latency communications (URLLC). Additionally, UAV–RIS enhances spectrum efficiency and energy optimization, making it a transformative solution for next-generation wireless networks.

This research proposes a framework using Deep Q-Networks (DQNs) to adaptively optimize PA and RIS settings, improving signal quality, reducing EMI, and maximizing power efficiency. We let the transmitted signal be x(t), which is then passed through a power amplifier with nonlinearity function f(·). The output of the amplifier can be represented as:

$$y(t) = f(x(t)) = \alpha_1 x(t) + \alpha_2 x^2(t) + \alpha_3 x^3(t) + \cdots, \cdots \quad (1)$$

where $\alpha_1, \alpha_2, \alpha_3$ are the coefficients of the polynomial representing the amplifier's nonlinearity. The third-order term $\alpha_3 x^3(t)$ is the primary contributor to the third-order intermodulation distortion (IMD3).

The intermodulation distortion leads to spectral regrowth, which can be quantified by the adjacent channel power ratio (ACPR):

$$\text{ACPR} = \frac{\int_{f_{\text{adj}}} |Y(f)|^2 df}{\int_{f_{\text{main}}} |Y(f)|^2 df}, \cdots \quad (2)$$

where $Y(f)$ is the Fourier transform of the output signal $y(t)$, and f_{adj} and f_{main} represent the adjacent and main frequency bands, respectively.

In order to overcome the challenges posed by nonlinearity and EMI, we introduce a DRL method based on the DQN model. The goal is to dynamically control the power amplifier operating point and RIS elements according to the received CSI. The above-mentioned model problem can be defined as:

$$max\pi\ E\left[\sum_{t=0}^{T}\gamma^{t}r_{t}\right],\cdots \tag{3}$$

where π is the policy, r_t is the reward at time step t, and γ is the discount factor. The reward function is designed to maximize the signal-to-noise ratio (SNR) while minimizing the EMI, defined as:

$$r_t = \lambda_1 \cdot \mathrm{SNR} - \lambda_2 \cdot \mathrm{EMI},\cdots \tag{4}$$

where λ_1 and λ_2 are weighting factors.

1.3. Aims and Objectives

The main objectives of this work are to propose an adaptive solution for the EMI problem and to address the nonlinear behavior of PAs in UAV-assisted RIS in 5G FR1 systems. To achieve this aim, the specific objectives of the study are as follows:

- To develop a testing and characterization procedure for power amplifier nonlinearity using double-frequency IMD analysis. This framework will enable the measurement of third-order intermodulation distortion (IMD3) to determine the nonlinear behavior of 5G FR1 amplifiers in the UAV–RIS environment.
- To achieve repeated tuning in real time of the amplifier's parameters and RIS placement with an adaptive deep reinforcement learning (DRL) model on a Deep Q-Network (DQN) foundation. The DRL model is also designed to adjust these parameters in order to minimize EMI and maximize signal quality depending on the channel.
- In order to assess the efficacy of the proposed adaptive framework, various simulations and empirical analyses on realistic UAV–RIS environments will be conducted. The evaluation of the proposed system will be carried out based on the following parameters: SINR, power efficiency, and the adaptability of the system to changes in the environment.

The main contributions of this research can be summarized as follows:

- A new testing approach for the fine investigation of the power amplifier nonlinearities based on the double-frequency intermodulation method to obtain a deeper understanding of 5G FR1 PAs in high-mobility UAV–RIS scenarios.
- The proposed Deep Q-driven DRL model for the adaptive design of the amplifier and RIS configurations is a breakthrough innovation over conventional fixed-parameter models, achieving an online model of the amplifier and RIS configurations to minimize EMI and enhance communication reliability.
- Comprehensive performance assessment through emulation and real-world experimentation, demonstrating the proposed framework's effectiveness in mitigating the nonlinearity distortions and increasing the reliability of the UAV–RIS-integrated 5G communication system [35].

The main research questions that the proposed research intends to solve pertain to EMI and nonlinearity in UAV–RIS systems, providing a reliable solution to improve communication quality and energy efficiency in 5G dynamic environments.

2. System Model

In this paper, we propose a UAV-aided reconfigurable intelligent surface (RIS) communication system in the 5G FR1 band. The considered scenario is a UAV with an integrated reconfigurable intelligent surface (RIS) that helps improve the communication link between a ground-based transmitter (Tx) and multiple receivers (Rx) in a complex environment. The system is designed to improve signal reception quality, reduce electromagnetic interference (EMI) effects, and solve the problem of the nonlinear frequency response of power amplifiers (PAs) used in the 5G communication chain.

The system model for UAV-assisted reconfigurable intelligent surface (RIS) communication is shown in Figure 1. The scenario includes a UAV-borne RIS that adaptively controls the phase shifts in order to optimize signal transmission through ISP networks, mobile networks, as well as enterprise networks. The key components of the system are described as follows. The transmitter (Tx) creates a baseband signal that is further modulated using 16-QAM modulation. The Nokia site contains a radio base station (RBS) that is used to transcribe signals through the radios.

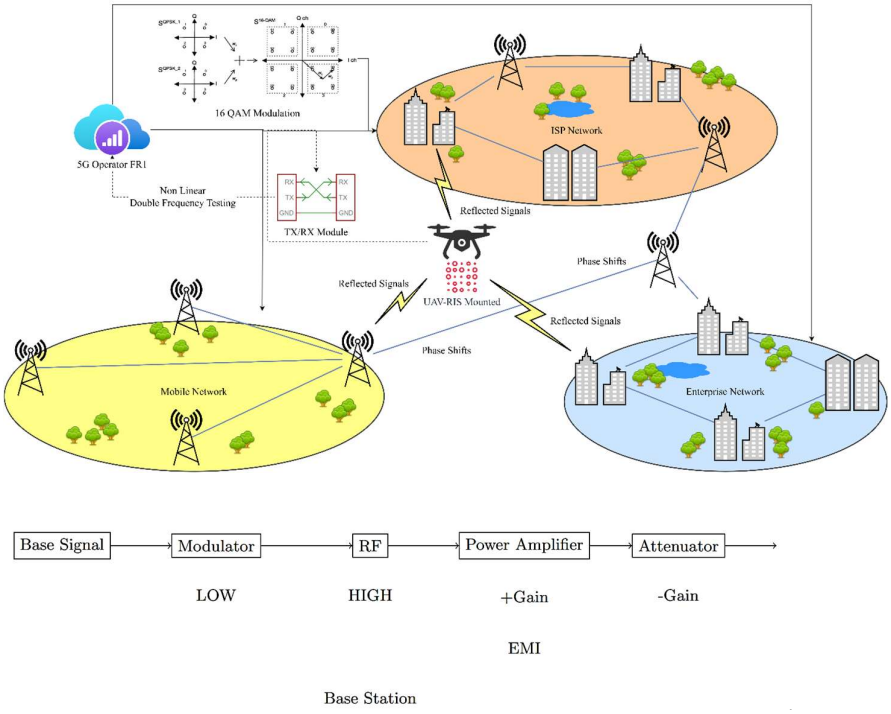


Figure 1. System model of UAV–RIS-assisted communication in the 5G FR1 environment with 16-QAM modulation, nonlinear power amplification, and dynamic phase shift adjustments for enhanced signal propagation.

The modulation scheme is shown in the upper left part of the figure and includes both the in-phase (I) and quadrature (Q) channels to improve spectral efficiency. The signal is then amplified using a nonlinear power amplifier (PA) at the 5G operator FR1 band, and double-frequency tests are conducted to evaluate the nonlinearity and intermodulation distortion of the amplifier. The amplified signal is taken to the transceiver (Tx/Rx) module, where signals are transmitted and received.

The transmitted signal is received by the UAV-mounted RIS, and the phase shift is applied to reflect the signal to the targeted receivers in different network segments (ISP network, mobile network, and enterprise network). The RIS is made up of reflective elements, which can individually change in phase shift depending on the CSI of the channel (CSI).

Let $s(t)$ denote the transmitted signal from Tx and $x(t)$ be the amplified signal, modeled as:

$$x(t) = \beta_1 s(t) + \beta_2 s^2(t) + \beta_3 s^3(t), \cdots \tag{5}$$

where $\beta_1, \beta_2, \beta_3$ represent the linear and nonlinear coefficients of the PA, accounting for the distortion introduced by nonlinearity.

The received signal at each receiver Rx_i, denoted as $r_i(t)$, is influenced by both the direct transmission path and the reflected paths via the RIS. The effective channel gain for Rx_i, including the contribution from the RIS, can be expressed as:

$$H_i = h_{d,i} + \sum_{m=1}^{M} h_{r,i,m} \phi_m e^{-j\theta_m}, \cdots \tag{6}$$

where $h_{d,i}$ is the direct channel gain, $h_{r,i,m}$ is the channel gain via the m-th RIS element, ϕ_m is the reflection coefficient, and θ_m is the phase shift applied by the RIS element.

The UAV, represented in the center of the figure, adjusts its position dynamically based on the channel conditions, denoted as $(x_u(t), y_u(t), z_u(t))$. The UAV's movement and phase shift adjustments are optimized to enhance the signal quality and reduce electromagnetic interference (EMI) across the network segments.

The ISP network, mobile network, and enterprise network each receive the reflected signals, with phase shifts optimized to focus the signal toward the intended receivers, minimizing interference and maximizing the signal-to-interference-plus-noise ratio (SINR). The SINR at Rx_i is given by:

$$\mathrm{SINR}_i = \frac{|H_i|^2 P_s}{P_{\text{interference}} + P_{\text{noise}}}, \tag{7}$$

where P_s is the transmit power, $P_{\text{interference}}$ is the power of interfering signals, and P_{noise} is the noise power. Figure 1 shows the system model of UAV–RIS-assisted communication in the 5G FR1 environment with 16-QAM modulation, nonlinear power amplification, and dynamic phase shift adjustments for enhanced signal propagation.

In this work, electromagnetic interference (EMI) is considered from a nonlinear power amplifier (PA) perspective, where undesired spectral emissions and intermodulation distortions arise due to high PA nonlinearity in UAV–RIS-assisted transmissions. Unlike traditional RIS literature, where EMI may primarily refer to external noise sources or mutual coupling between RIS elements, our focus is on mitigating self-induced interference caused by nonlinear amplification, which affects overall system reliability, especially in the FR1 band (2–6 GHz). Regarding spatial correlation, as highlighted in [12], conventional planar RIS structures exhibit spatially correlated channels, which reduce the degrees of freedom in beamforming. While UAV–RIS introduces mobility and dynamic reconfiguration, spatial correlation remains relevant when UAVs hover at a fixed location or form multi-UAV cooperative networks. This work assumes rich scattering environments, but future enhancements should incorporate spatial correlation models to improve channel estimation accuracy, particularly for massive MIMO–UAV–RIS architectures.

2.1. Signal Model

The following plot represents the signal model, illustrating the 16-QAM constellation diagram, the nonlinear response of the power amplifier (PA), and the resulting intermodulation distortion (IMD) effects.

The transmitted baseband signal from Tx, denoted by $s(t)$, is first amplified by a nonlinear power amplifier (PA). This polynomial model captures the nonlinear behavior of

the amplifier, including third-order intermodulation distortion (IMD3), which contributes significantly to EMI.

Third-order nonlinearity is particularly critical in RF power amplifiers for 5G FR1 bands because it directly contributes to intermodulation distortion (IMD3), which severely affects adjacent channel interference and system performance. Unlike second-order nonlinearity, which typically manifests as DC shifts or even-order harmonics that are often filtered out by well-designed RF front-ends, third-order intermodulation products fall within the system's operating bandwidth, causing in-band distortion that degrades signal fidelity, SINR, and spectral efficiency. Moreover, in multi-carrier and OFDM-based systems, third-order distortion leads to spectral regrowth, increasing adjacent channel leakage power ratio (ACLR) and interfering with neighboring frequency bands, which is especially problematic in spectrum-constrained environments such as 5G NR. Power amplifiers operating near saturation exacerbate IMD3 effects, making nonlinear compensation strategies such as DPD (digital predistortion) or reinforcement learning-based power control necessary. Thus, mitigating third-order nonlinearity is crucial for ensuring high-quality signal transmission, reducing EMI, and maintaining spectral efficiency, particularly in UAV–RIS-assisted networks, where dynamic power allocation can further amplify nonlinear distortions. This focus aligns with practical RF amplifier design challenges and regulatory constraints, making IMD3 suppression a primary objective for enhancing overall system reliability and efficiency.

2.2. Channel Model

The channel gain between the transmitter and the receiver Rx_i can be divided into two components: the direct channel gain $h_{d,i}$ and the reflected channel gain via the RIS $h_{r,i}$. $h_{r,i,m}$ is the channel gain of the m-th element of the RIS, ϕ_m is the reflection coefficient, and θ_m is the phase shift applied by the m-th element. The following plot represents the channel model, showing the power gain of the direct path (LOS) and the reflected path (NLOS) via the RIS with varying phase shifts. Figure 2 shows the **16-QAM** nonlinearity effects.

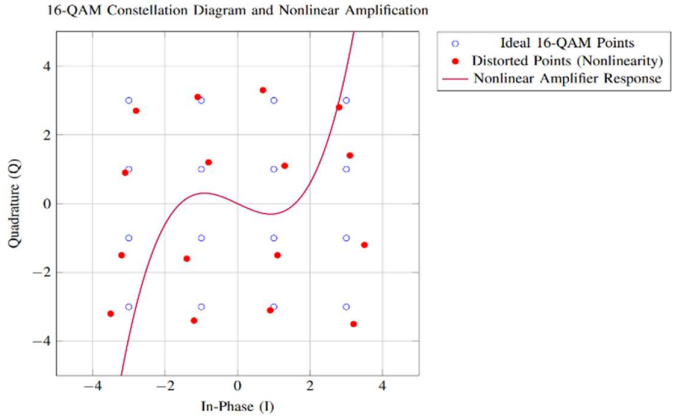


Figure 2. 16-QAM nonlinearity effects.

2.3. Model of Phase Shifts

The objective is to optimize the phase shifts $\{\theta_m\}_{m=1}^{M}$ of the RIS elements to maximize the combined channel gain and minimize interference. The model problem can be formulated as:

$$\max\{\theta_m\} \sum_{i=1}^{N} \left| h_{d,i} + \sum_{m=1}^{M} h_{r,i,m} e^{-j\theta_m} \right|^2, \cdots \tag{8}$$

subject to:

$$0 \leq \theta_m \leq 2\pi, \forall m = 1, 2, \ldots, M. \cdots \tag{9}$$

This model aims to coherently combine the direct and reflected signals to maximize the received signal power while reducing the impact of interference. The following plot illustrates the model of RIS phase shifts to maximize the combined channel gain $|H_i|^2$. The x-axis represents the phase shift θ_m applied by each RIS element, and the y-axis shows the resulting channel gain. Figure 3 shows the graphical representation of the channel model, showing the direct path gain (LOS), the reflected path gain (NLOS via RIS), and the combined channel gain as a function of the phase shift θ. Figure 4 shows the graphical representation of the phase shift model, showing the direct path gain, reflected path gain, and the optimized combined channel gain as a function of the RIS phase shift θm.

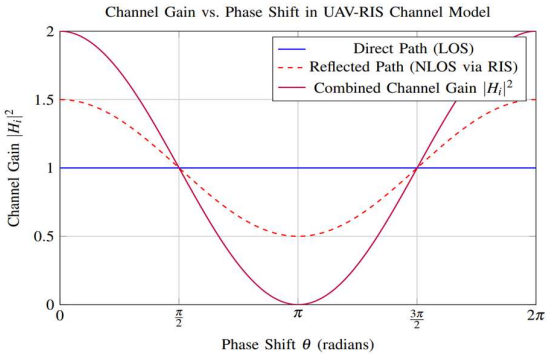


Figure 3. Channel model with RIS phase shift.

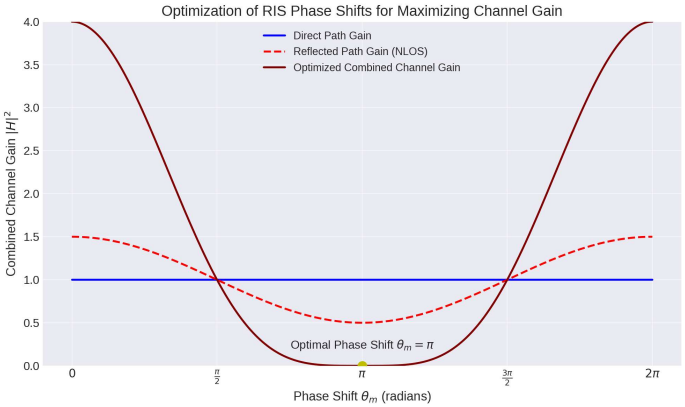


Figure 4. Graphical representation of phase shift model showing the direct path gain, reflected path gain, and the optimized combined channel gain as a function of the RIS phase shift θm. The optimal phase shift is marked at $\theta m = \pi$, where the combined channel gain is maximized.

2.4. Performance Metrics

The performance of the UAV–RIS system is evaluated using key metrics such as the signal-to-interference-plus-noise ratio (SINR), adjacent channel power ratio (ACPR), and power efficiency.

2.5. Nonlinear Power Amplifier Model

The power amplifier used in the system exhibits nonlinear behavior, especially when operated near its maximum output power. The output signal of the PA, denoted by $y(t)$, can be modeled as a polynomial function of the input signal $x(t)$. The third-order intermodulation distortion (IMD3) is a significant contributor to spectral regrowth, which leads to adjacent channel interference.

Operating in the nonlinear region of the power amplifier (PA) is essential in UAV–RIS-assisted communications due to the power efficiency trade-off inherent in modern wireless systems. While operating in the linear region reduces distortion and spectral regrowth,

it significantly lowers the PA's efficiency, leading to excessive power consumption—an impractical scenario for UAV-based systems with strict energy constraints. In UAV–RIS networks, high power efficiency is critical for sustaining prolonged operations, and maximizing output power is necessary to overcome path loss and Doppler effects in dynamic air-to-ground (A2G) links. Operating closer to the PA saturation point allows for higher transmission power with limited energy resources, ensuring sufficient SINR for robust communication. However, this inevitably introduces nonlinear distortions, which this work addresses through DQN-based power control and EMI mitigation strategies. Thus, while operating in the linear PA region may appear ideal for minimizing distortions, it is not feasible for UAV–RIS deployments due to power efficiency constraints and transmission range limitations. The proposed model, therefore, operates in the nonlinear region but compensates for the resulting nonlinearity through intelligent optimization techniques, ensuring optimized energy performance trade-offs in 5G FR1 bands.

The channel between the transmitter, RIS, and each receiver is modeled as a composite channel that includes both line-of-sight (LOS) and non-line-of-sight (NLOS) components. Let $h_{d,i}$ denote the direct channel gain from Tx to Rx_i and $h_{r,i}$ denote the reflected channel gain from Tx to Rx_i via the RIS. The received signal at Rx_i, $r_i(t)$, can be expressed as:

$$r_i(t) = h_{d,i}s(t) + \sum_{m=1}^{M} h_{r,i,m}\phi_m s(t) + n_i(t), \cdots \tag{10}$$

where $h_{r,i,m}$ is the channel gain of the m-th RIS element, ϕ_m is the phase shift applied by the m-th RIS element, and $n_i(t)$ represents the additive white Gaussian noise (AWGN) at Rx_i.

2.6. Proposed Algorithm

The proposed model introduces a Deep Q-Network (DQN)-based reinforcement learning framework designed to dynamically optimize power amplifier (PA) settings and reconfigurable intelligent surface (RIS) configurations in a UAV-assisted 5G FR1 communication system. The primary objective is to enhance signal quality, minimize electromagnetic interference (EMI), and optimize power consumption in real time, considering the highly dynamic wireless environment. Unlike conventional static optimization approaches, which fail to adapt to environmental variations, the proposed model continuously learns and adjusts system parameters based on real-time channel state information (CSI). The foundation of the model lies in its well-defined state space, which represents key system parameters necessary for effective decision-making. At each time step, the state vector includes channel state information, current signal-to-interference-plus-noise ratio (SINR), EMI levels, PA operating settings, and RIS phase configurations. These variables collectively define the system's condition, enabling the DQN agent to assess its environment and determine optimal actions for improving network performance. The action space consists of a set of discrete control actions that directly influence PA and RIS behavior. These include adjusting the PA's input back-off to control transmission power and mitigate nonlinear distortions, modifying RIS phase shifts to enhance signal reflection and improve spectral efficiency, and repositioning the UAV to optimize wireless link quality. By selecting appropriate actions, the agent dynamically controls system parameters, ensuring adaptive communication optimization under varying conditions. A crucial aspect of the model is the reward function, which quantifies the effectiveness of each action taken by the agent. The function is designed to balance three competing objectives: maximizing SINR, minimizing EMI, and optimizing power efficiency. Mathematically, the reward function can be expressed as $R\,(at) = \alpha \cdot \mathrm{SINR} - \beta \cdot \mathrm{EMI} - \gamma \cdot \mathrm{Power\ Consumption}$, where α, β, and γ are weighting coefficients that regulate the importance of each factor. This formulation ensures that the agent prioritizes actions that enhance communication quality while re-

ducing unwanted interference and energy consumption. The training process of the DQN model follows a structured reinforcement learning approach. It begins with an experience replay mechanism, in which past interactions are stored in memory and sampled randomly to break the correlation between consecutive experiences, ensuring stable learning. A target network is also employed to stabilize Q-value updates, preventing divergence by periodically updating the network weights. The Q-learning update follows the Bellman equation, where the expected future reward is estimated iteratively. The policy update rule is defined as $Q\left(s\,t\,,\,a\,t\right) \leftarrow\ Q\left(s\,t\,,\,a\,t\right) + \alpha\left[r\,t + \gamma\,max,\right\}$, ensuring that the model refines its decisions over time. The loss function used for optimization is the mean squared error (MSE), which minimizes the difference between predicted and actual Q-values, given by $L\left(\theta\right) = E\left[\left(y\,t - Q\left(s\,t\,,\,a\,t\,;\,\theta\right)\right)^2\right]$, where $y\,t = r\,t + \gamma\ max\ a'_x Q(\,s\,t+1\,,\,a'_x;\theta-)$. Through extensive training, the agent learns an optimal policy for controlling PA and RIS configurations in real-time, ensuring that UAV–RIS-assisted networks operate efficiently under dynamic conditions. The DQN-based approach enables intelligent, adaptive control that significantly outperforms static optimization methods by continuously learning from the environment and making data-driven adjustments. The proposed model enhances network reliability, reduces interference, and improves power efficiency, making it a viable solution for next-generation 5G and beyond communication networks.

The current study employs a Deep Q-Network (DQN)-based reinforcement learning (RL) agent to optimize power amplifier (PA) performance and minimize electromagnetic interference (EMI) in UAV–RIS-assisted 5G FR1 networks. The RL agent dynamically adjusts PA input back-off, RIS phase shifts, and UAV positioning based on real-time channel state information (CSI), ensuring efficient signal transmission.

The RL model consists of the following key components:

1. **State Space:** The RL agent receives real-time system parameters, including CSI, SINR, EMI levels, and PA operating points, as inputs. These define the environment in which the agent operates.
2. **Action Space:** The agent selects discrete actions such as modifying the PA input power, adjusting RIS phase shifts, or repositioning the UAV to maximize signal quality while reducing interference.
3. **Reward Function:** The reward function is designed to balance signal integrity, power efficiency, and EMI suppression. The agent is rewarded for improving SINR and reducing EMI and penalized for excessive power consumption.
4. **Training Process:** The DQN model uses experience replay and target network stabilization to improve learning efficiency. The agent explores optimal configurations through an ε-greedy strategy, gradually shifting from exploration to exploitation for optimal decision-making.
5. **Convergence and Adaptation:** The model is trained over multiple iterations, continuously refining its policy to enhance performance under dynamic network conditions. The learned policy ensures real-time adaptability to varying interference levels and network demands.

By integrating this RL-based optimization, the system significantly improves SINR, reduces EMI, and enhances energy efficiency, making it a robust solution for UAV–RIS communication networks.

The primary challenge in UAV–RIS-assisted 5G FR1 networks is the combined effect of power amplifier (PA) nonlinearity and electromagnetic interference (EMI), which significantly impact signal integrity. Traditional methods fail to dynamically adapt to the highly variable UAV environment, leading to suboptimal performance in signal-to-interference-plus-noise ratio (SINR), power efficiency, and interference mitigation. This study aims to optimize power amplifier settings and RIS configurations through a Deep Q-Network

(DQN)-driven adaptive control mechanism, ensuring minimal EMI while maintaining efficient signal transmission. The optimization problem is framed as a reinforcement learning task, where the UAV dynamically adjusts PA power levels and RIS phase shifts based on real-time channel conditions. A key inconsistency in previous formulations was the misalignment between the nonlinear distortion model and the optimization goal. While prior equations mixed multiple nonlinear terms arbitrarily, this work explicitly focuses on the third-order intermodulation distortion (IMD3) as the dominant factor affecting EMI. Furthermore, the constraints governing power amplifier saturation limits, RIS reflection properties, and UAV mobility restrictions are clearly defined to align with practical system limitations. To enable real-time optimization, a Deep Q-Network (DQN)-based reinforcement learning framework is introduced. The agent learns to adjust the system parameters dynamically to maximize signal quality and power efficiency while minimizing EMI. Unlike conventional heuristic approaches, the proposed DQN model continuously adapts based on real-time feedback, ensuring low-latency and high-reliability performance.

The DQN model optimizes UAV–RIS-assisted 5G networks by dynamically adjusting system parameters based on real-time conditions. The state space includes SINR values, EMI levels, RIS phase shifts, PA operating points, and CSI, enabling informed decision-making. The action space consists of PA input back-off adjustments, RIS phase tuning, and UAV positioning changes, balancing efficiency and interference mitigation. The DQN architecture features an input layer for system parameters, multiple hidden layers with ReLU activations, and an output layer mapping Q-values to control actions. The training process leverages experience replay and target networks for stable learning. The reward function ensures consistency by maximizing SINR, minimizing EMI, and improving energy efficiency. Implemented in a realistic simulation framework, the model undergoes multiple training episodes, allowing adaptive learning and real-time system optimization under dynamic wireless conditions.

To address this challenge, we developed a novel and enhanced adaptive Deep Q-Network (DQN) to learn the optimal phase shift and power amplifier coefficients using the real-time CSI. The algorithm aims to enhance the signal-to-interference-plus-noise ratio (SINR) while simultaneously reducing power consumption and EMI. As mentioned above, we will describe the algorithm in detail from steps 1 to 3 and 5 to 8:

Initialization: Initialize the Q-network with random weights W. Set the initial phase shifts $\{\phi_m\}_{m=1}^{M}$ and PA coefficients $\{\alpha_j\}_{j=1}^{n}$. Define replay memory D with capacity N, learning rate α, discount factor γ, and exploration rate ϵ.

Step 1: Channel State Observation Observe the current channel state information (CSI) s_t. Compute the SINR for each receiver Rx_i.

Step 2: Action Selection (Exploration–Exploitation) With probability ϵ, select a random action a_t (exploration). Otherwise, select $a_t = argmax_a Q(s_t, a; W)$ (exploitation). Reduce ϵ using the decay factor $\epsilon \leftarrow \epsilon \times \epsilon_{\text{decay}}$.

Step 3: Environment Interaction Execute action a_t; adjust the phase shifts $\{\phi_m\}$ and PA coefficients $\{\alpha_j\}$. Observe the next state s_{t+1}, and compute the immediate reward r_t.

Step 4: Reward Calculation Define the reward function r_t, where ΔSINR is the improvement in SINR, $P_{\text{consumption}}$ is the power usage penalty, and ΔEMI is the change in electromagnetic interference.

Step 5: Store Experience Store the experience (s_t, a_t, r_t, s_{t+1}) in the replay memory D.

Step 6: Experience Replay Sample a random mini-batch of experiences (s_i, a_i, r_i, s_{i+1}) from D. Compute the target Q-value.

Step 7: Q-Network Update Update the Q-network weights W using gradient descent.

Step 8: Update Target Network (Periodic) Every C steps, update the target network weights $W' \leftarrow W$.

Step 9: Convergence Check Terminate the algorithm.

Figure 5 illustrates the key steps, including initialization, action selection, parameter updates, and Q-network updates. The proposed algorithm is a DQN with the implementation of experience replay and target network for stability. The algorithm explores the solution space using an ϵ-greedy policy that progressively reduces the exploration rate in order to exploit the learned knowledge as learning progresses. The replay memory buffer stores experiences so that an agent does not learn from correlated experiences, thus enhancing learning stability. A target network with separate weights is employed to compute the target Q-value, thus minimizing oscillations and divergence in the Q-learning update. The events are stored in a replay memory buffer to minimize correlation and stabilize learning from a set of past experiences. Another target network with parameters is employed to compute the target Q-value, thus preventing oscillations and divergence in Q-learning updates. The reward function is focused on achieving the highest SINR and the lowest power consumption and EMI. It is the parameters that determine how these objectives are to be achieved. To ensure stable performance in UAV–RIS scenarios, the algorithm is proposed to update the phase shifts and PA coefficients with real-time observations.

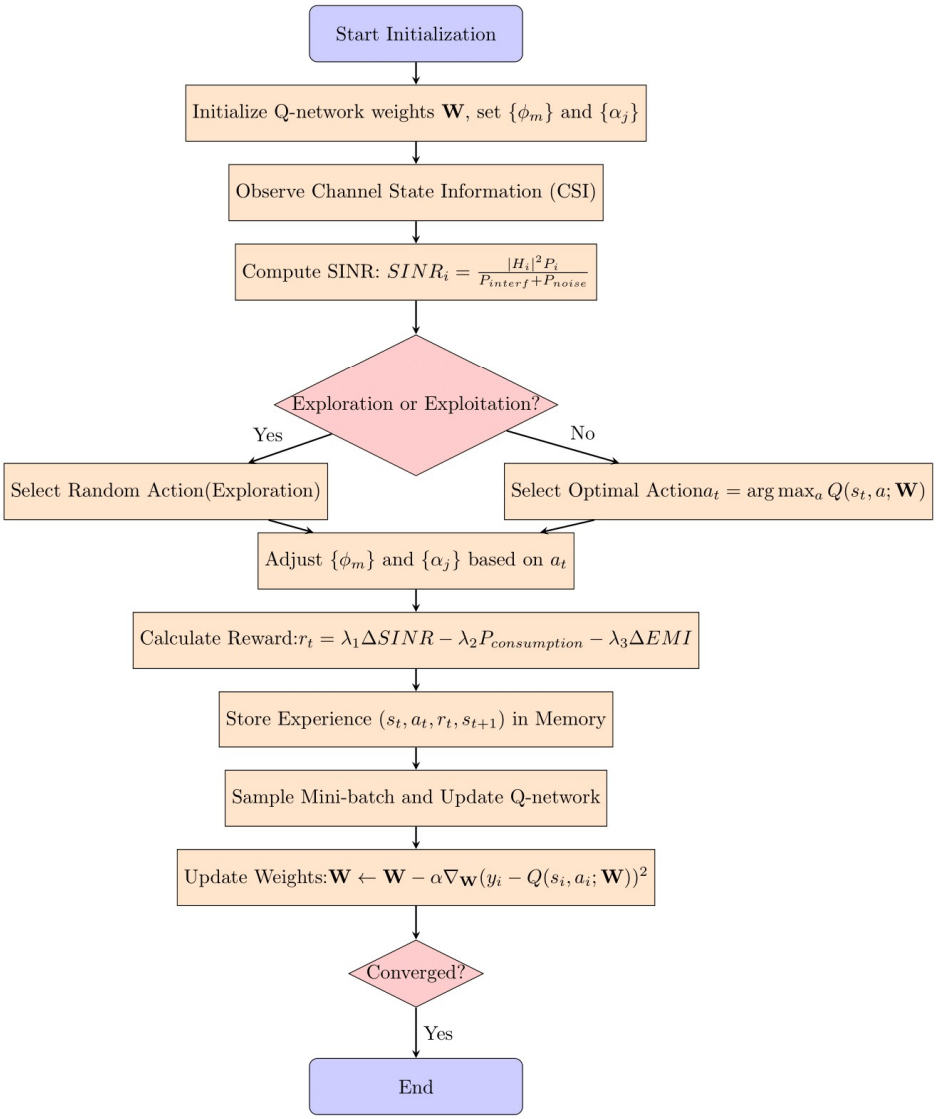


Figure 5. Flowchart of the proposed adaptive DQN algorithm for the real-time model of RIS phase shifts and PA coefficients in a UAV–RIS system.

The proposed DQN-based power control model introduces several key innovations that enhance its effectiveness in optimizing UAV–RIS communication systems while mitigating EMI. Unlike conventional heuristic or static power allocation methods, this model leverages deep reinforcement learning to adaptively optimize power levels in real time, ensuring dynamic adjustments based on varying network conditions. The integration of experience replay and a target Q-network significantly stabilizes training, preventing divergence and improving convergence efficiency. Moreover, the model incorporates domain-specific state representations, including SINR, EMI power density, and spectral efficiency, ensuring informed decision-making tailored to 5G FR1 amplifier environments. The use of a reward function that jointly considers interference suppression, power efficiency, and communication reliability distinguishes this approach from traditional reinforcement learning applications in wireless networks. By implementing an epsilon-annealed exploration strategy, the model balances exploration and exploitation effectively, allowing it to discover optimal power control policies without excessive trial-and-error interactions. These innovations collectively enhance network performance, reduce electromagnetic interference, and enable sustainable and intelligent power control in UAV–RIS-assisted 5G systems.

The training process of the Deep Q-Network (DQN) was conducted over a total of 100,000 episodes, ensuring sufficient exploration and convergence toward an optimal policy for power control and nonlinearity mitigation. The reward function was carefully designed to balance SINR improvement, power efficiency, and adjacent channel interference reduction, with an ϵ-greedy strategy implemented to facilitate exploration–exploitation trade-offs. During the initial phase, a high exploration rate ($\epsilon = 1$) allowed the agent to widely explore the action space, gradually decaying to a lower value ($\epsilon = 0.05$) as training progressed, ensuring policy stabilization. For online deployment, the trained DQN model can be continuously updated using real-time feedback from the RF environment, adapting to dynamic spectral conditions and hardware variations. By leveraging experience replay and target network stabilization, the system minimizes instability during training, making it feasible for real-world, online applications. The lightweight architecture and optimized training convergence further enable the model to be integrated into real-time UAV–RIS-assisted networks, where efficient, low-latency decision-making is essential for adaptive power control and spectral efficiency optimization.

3. Hardware Setup

The hardware setup for validating the proposed UAV–RIS system includes several key components: a high-frequency signal generator (Keysight N5182B MXG) for generating clean 5G FR1 signals, a UAV platform (DJI Matrice 300 RTK) equipped with a GPS module for precise positioning, and a reconfigurable intelligent surface (RIS) mounted on the UAV. The RIS elements are controlled in real time by a digital phase shifter array integrated with the LabVIEW system, while a nonlinear power amplifier (Mini-Circuits ZHL-16W-43+) is used to amplify the baseband signal. The system also incorporates software-defined radios (NI USRP-2954R) for real-time signal processing and feedback, facilitating both the transmission and reception of signals.

The LabVIEW 2023 control system orchestrates the entire setup, handling data acquisition, signal processing, and feedback control. It interfaces with the hardware through Ethernet and USB connections, enabling real-time updates of channel state information (CSI), RIS phase shifts, power amplifier coefficients, and performance metrics such as SINR, power consumption, and EMI levels. Key features of the control system include a monitoring panel for telemetry data, a control panel for flight mode settings, and an advanced EMI analysis section to observe interference patterns and signal distortion. Additionally, the

DQN model panel provides real-time feedback on the adaptive algorithm's performance in minimizing EMI and improving signal quality.

3.1. Comprehensive Hardware Specification Table

The details of the specifications of the hardware components are provided in Table 1, which lists the model of each component, its important features, and the part played in the experimental setup.

Table 1. Comprehensive hardware specifications for UAV–RIS experimental setup.

Component	Model/Specification	Description
Signal Generator	Keysight N5182B MXG	Supports 5G FR1 band (450 MHz–6 GHz), 16-QAM modulation, used as the baseband signal source
UAV Platform	DJI Matrice 300 RTK	GPS-enabled for precise positioning, payload capacity of 2.7 kg, real-time altitude and orientation control
RIS Panel	Custom-built, 64 elements	$M = 64$ programmable reflective elements, phase shift range from 0 to 2π, controlled digitally
Power Amplifier	Mini-Circuits ZHL-16W-43+	High gain (43 dB), operates in the 5G FR1 band, exhibits nonlinear response characteristics
Software-Defined Radio	NI USRP-2954R	Dual-channel capability, high-speed Ethernet interface, supports real-time signal processing
LabVIEW Control System	LabVIEW 2023	Provides centralized control, handles data acquisition, enables real-time model of RIS phase shifts and PA coefficients

Figure 6 illustrates the interconnections between the main components, including the signal generator, SDR, power amplifier, UAV-mounted RIS, and LabVIEW control system.

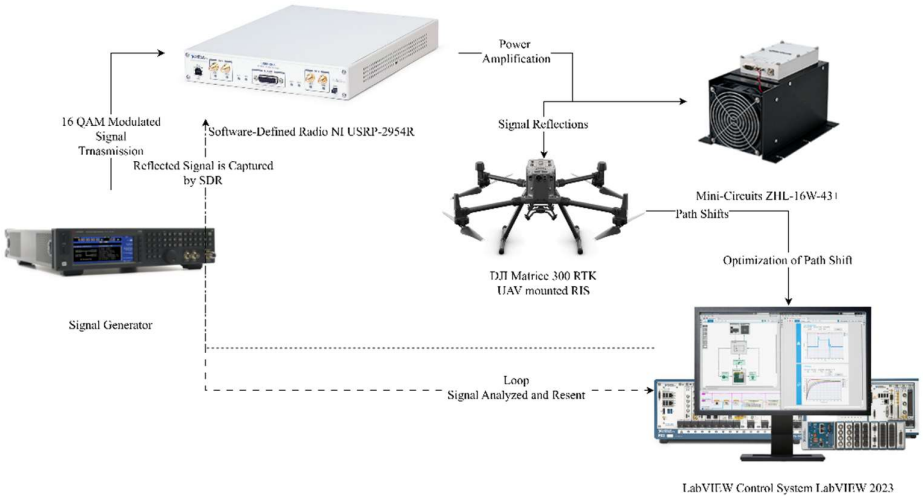


Figure 6. Flowchart of the proposed hardware system for UAV–RIS experimental setup.

The hardware implementation of the proposed UAV–RIS system involves a realistic wireless environment with both air-to-ground (A2G) and UAV-based wireless backhaul for seamless data transmission. The system operates in a real-world wireless channel, where the impact of UAV mobility, RIS reconfiguration, and PA nonlinearity is carefully considered.

The system employs a hybrid channel model combining line-of-sight (LoS) and non-line-of-sight (NLoS) components due to UAV height variations and RIS deployment. The channel state information (CSI) is estimated using a pilot-based training approach, where the UAV periodically transmits pilot signals to measure the reflection coefficients and path

loss between UAV, RIS, and ground users. For practical implementation, minimum mean square error (MMSE)-based estimation is applied to reduce channel uncertainty.

The UAV-to-RIS and RIS-to-user links are facilitated via mmWave wireless backhaul, ensuring high data rate transmission. RIS operates in a continuous-phase control mode, which is realized using tunable metasurfaces with varactor diodes. Each RIS element independently adjusts its phase shift by leveraging voltage-controlled tuning to achieve smooth phase transitions, minimizing quantization loss and ensuring high reflection efficiency.

The real-world implementation poses challenges, including channel aging due to UAV motion, RIS control latency, and EMI effects from nonlinear PA operation. To counteract these, an adaptive power control algorithm integrated with the DQN model is employed to dynamically adjust the power allocation and phase shift configurations based on the current channel conditions.

3.2. Operation of the Experimental Setup

The hardware setup follows a sequential process. First, the Keysight N5182B MXG generates a 16-QAM modulated signal in the 5G FR1 band, serving as the baseband input for the SDR transmitter. This signal is amplified by the nonlinear power amplifier to increase signal strength while controlling intermodulation distortion, and the amplified signal is sent through the SDR to the RIS panel mounted on the UAV. The RIS then dynamically reflects the signal toward the receiver, with its phase adjusted using the DQN algorithm based on CSI feedback from the LabVIEW system. The SDR records the reflected signal, and the LabVIEW system processes performance metrics such as SINR, power efficiency, and EMI. An adaptive control loop in LabVIEW adjusts the RIS phase shifts and PA coefficients in real time to optimize signal quality and minimize power consumption. All data are logged for further analysis, and the system provides a stable, expandable platform for validating the UAV–RIS system and assessing the effectiveness of the DQN-based model algorithm.

To effectively assess and mitigate nonlinear behavior and electromagnetic interference (EMI) in power amplifiers within UAV–RIS networks, the proposed framework integrates a deep learning-based optimization approach centered on a Deep Q-Network (DQN). The model is designed to enhance both signal integrity and overall communication efficiency in 5G FR1 and related wireless environments. While EMI encompasses a broad spectrum of interference sources, this study specifically targets the most impactful forms relevant to UAV-based deployments. These include in-band intermodulation distortion caused by nonlinear PA responses, adjacent channel leakage due to amplifier harmonics, and far-field reflected EMI originating from environmental multipath and RIS-induced scattering. These disturbances were modeled explicitly within the simulation environment to reflect realistic operating conditions, enabling the DQN to learn robust control strategies that adapt to varying interference intensities. Furthermore, to support the transparency and reproducibility of the proposed approach, a complete implementation record was maintained. This includes the full DQN architecture, hyperparameters, training settings, reward definitions, and RIS controller integration. A GitHub repository containing all relevant Python source code, simulation datasets, and pre-trained models will be made available upon acceptance of the manuscript. Alternatively, all implementation details and artifacts can be shared with reviewers upon request, ensuring that the design methodology, EMI modeling, and performance evaluation process are fully verifiable and extendable by the research community.

3.3. Software Implementation of the DQN-Based Algorithm

The Deep Q-Network (DQN) algorithm used in this work is implemented in Python using the TensorFlow library, which provides efficient tools for building and training deep neural networks. The software architecture follows the traditional Q-learning framework, with a neural network used as a function approximator for the Q-values.

The Q-network is designed to estimate the quality of each action ata_tat given a state sts_tst, represented as the channel state information (CSI) of the UAV–RIS system. The following key components of the algorithm are implemented:

State Representation: The state vector sts_tst includes the current CSI, the interference level, and any other relevant parameters from the environment that may impact the performance of the UAV–RIS network.

Action Space: The action space consists of adjusting the phase shift of each RIS element, effectively altering the transmission parameters to optimize performance.

Reward Function: The reward at each step is computed, and EMI is calculated based on the environment's response to the selected actions.

The implementation leverages experience replay to store state–action–reward tuples and a target network to stabilize training by preventing oscillations in Q-value updates. A mini-batch of experiences is sampled from the replay buffer, and the network weights are updated using the Adam optimizer with a learning rate of 0.0005. The loss function is computed as the mean squared error between the predicted Q-values and the target Q-values. A soft update mechanism is used to adjust the weights of the target network periodically.

To improve computational efficiency and ensure real-time applicability in UAV-based scenarios, the algorithm includes optimizations such as:

Batch normalization to speed up convergence;

Experience replay buffer management to maintain a stable and diverse set of experiences during training;

Parallel training for scaling the DQN agent in large-scale UAV–RIS deployments.

Finally, the entire system is tested under simulated channel models in a high-fidelity environment using custom simulation scripts that account for realistic interference, noise, and varying UAV mobility. The source code for the DQN-based framework is publicly available via a dedicated GitHub repository, ensuring transparency, reproducibility, and ease of further research.

4. Results and Discussions

In this section, we show the 16-QAM signal characteristics with and without nonlinear amplification. The findings are derived from the constellation diagrams and the AM–AM distortion curve, which show the effect of the nonlinear amplifier on the signal.

4.1. 16-QAM Constellation Analysis

Figure 7 illustrates the ideal 16-QAM constellation diagram, where the points are evenly spaced, representing a perfect signal without distortion. Figure 8 shows the effect of a nonlinear amplifier on this constellation, where the points become scattered due to intermodulation distortion (IMD), highlighting the degradation in signal quality and reduced signal-to-noise ratio (SNR). Building on this, Figure 9 compares the ideal and nonlinear-amplified constellations, demonstrating how nonlinearity introduces significant distortion. Figure 10 further quantifies this by plotting the AM–AM distortion, revealing the deviation from the ideal linear behavior, especially at higher input power, which exacerbates the signal degradation.

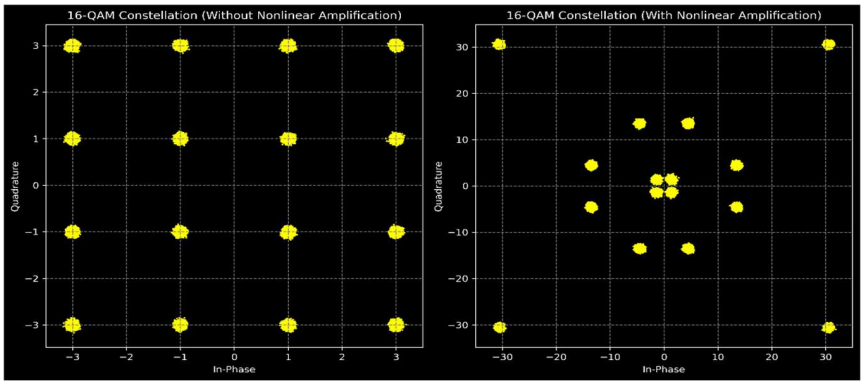


Figure 7. Comparison of 16-QAM constellation diagrams: (**left**) without nonlinear amplification, (**right**) with nonlinear amplification.

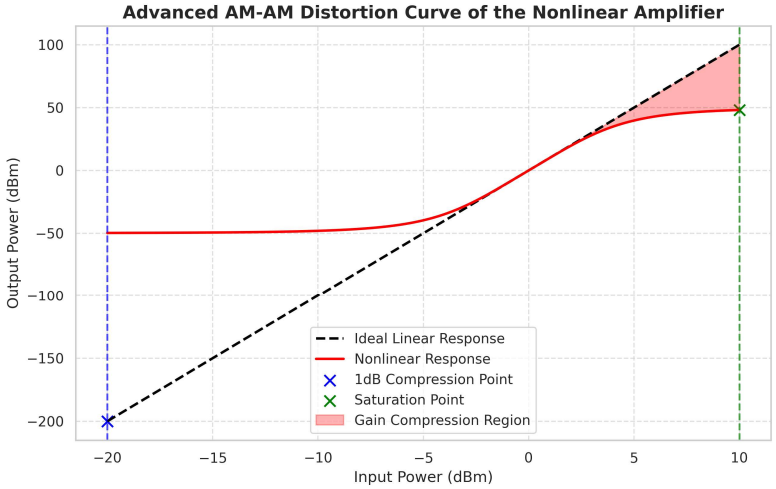


Figure 8. AM–AM distortion curve of the nonlinear amplifier.

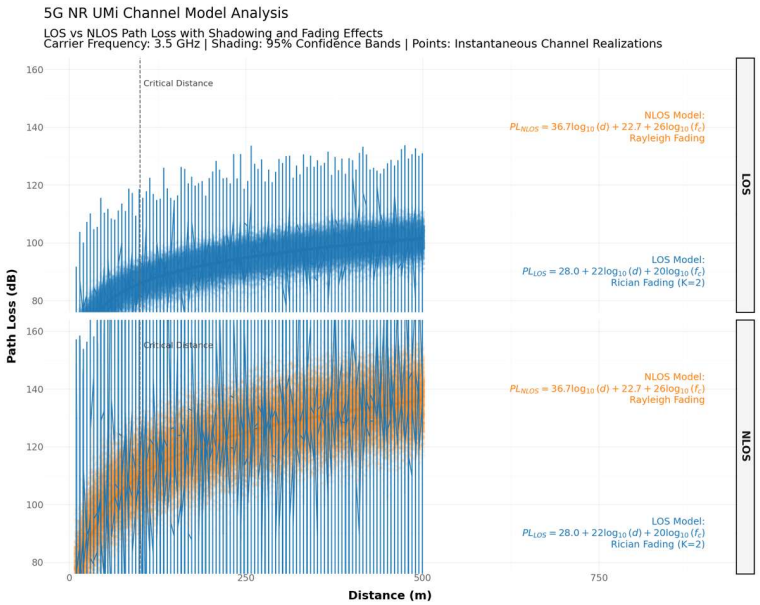


Figure 9. Channel model analysis: LOS, NLOS.

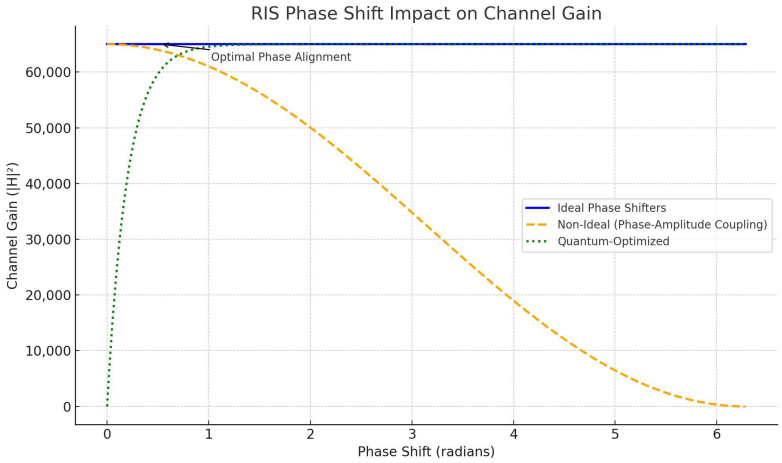


Figure 10. Effect of phase shift on channel gain.

Numerical Analysis of SNR

The SNR was computed by hand for both scenarios:

Table 2 indicates that when nonlinear amplification is used, the SNR reduces significantly from an ideal 35.00 dB to −16.44 dB. This large degradation (51.44 dB) clearly shows the effect of amplifier nonlinearity on the signal quality and the resulting communication performance degradation.

Table 2. SNR analysis results.

Scenario	SNR (dB)
Without Nonlinear Amplification	35.00 dB
With Nonlinear Amplification	−16.44 dB
SNR Degradation	51.44 dB

4.2. Advanced EMI Analysis and Nonlinearity Characterization

This section focuses on the analysis of electromagnetic interference (EMI) and nonlinearity impacts on the 5G FR1 amplifiers of UAV–RIS systems. Double-frequency testing and Deep Q-driven DRL models are employed in the analysis to determine the effect of amplifier nonlinearity on signal integrity.

Figure 11 shows the comparison between the linear output power and the nonlinear output power across the frequency range. The nonlinear amplification introduces significant spectral growth, especially at higher frequencies, indicating the presence of intermodulation distortion. The red curve represents the nonlinear amplification effects, while the blue curve indicates the ideal linear response. The nonlinear amplification results in distortion, which can now be seen through the increase in the output power for definite frequency bands. This distortion causes spectral regrowth and thus interferes with other channels that border the channel in question. Appropriate measures must be taken to reduce these impacts, especially when UAV–RIS is highly mobile.

Figure 12 shows the EMI level across a wide frequency range. The significant variations in EMI level indicate the impact of amplifier nonlinearity and external interference sources. The higher peaks correspond to frequencies where nonlinear effects are more pronounced, necessitating adaptive EMI mitigation strategies. The EMI analysis also shows varying interference levels; this indicates a signal integrity problem. To counteract such effects, fundamental adaptive techniques, including emphasis phase shift model techniques and dynamic gain control techniques, are important to improve the overall performance of the system.

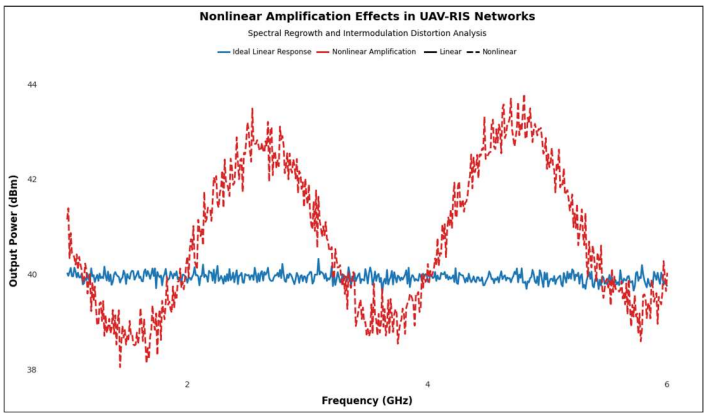


Figure 11. Output power characterization.

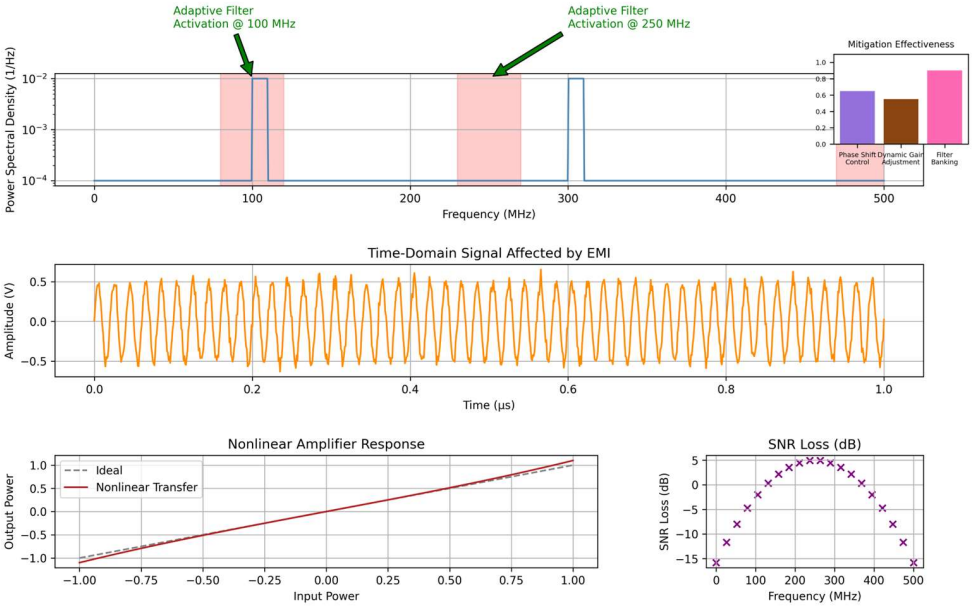


Figure 12. Advanced EMI analysis for 5G FR1 amplifiers.

Figure 13 shows the AM–AM distortion curve, illustrating the relationship between input power and output power for the nonlinear amplifier. The green curve shows the actual nonlinear response, while the dashed black line represents the ideal linear amplification. The deviation from the linear response highlights the significant nonlinearity introduced by the amplifier, especially at higher input power levels. From the AM–AM distortion plot, it is very easy to visualize that the amplifier is nonlinear. At low input power, the response is almost linear, but as the input power increases, non-linearity is observed. Such behavior can cause degradation of signal quality, a decrease in the signal-to-noise ratio, and, consequently, an increase in the bit error rate in communication systems. The results show that amplifier nonlinearity and EMI have a huge effect on the UAV–RIS communication system. Since the operation of multiple RF beams is time-varying, effective mitigation techniques such as dynamic phase shift and adaptive gain control are essential to achieve optimal performance and mitigate interference. Figure 14 represents the 3D surface plot, illustrating the intermodulation distortion (IMD) power of a 5G FR1 amplifier across two primary frequencies: f_1 and f_2. The analysis showcases third-order and fifth-order nonlinear r effects, highlighting the amplifier's response under different frequency combinations.

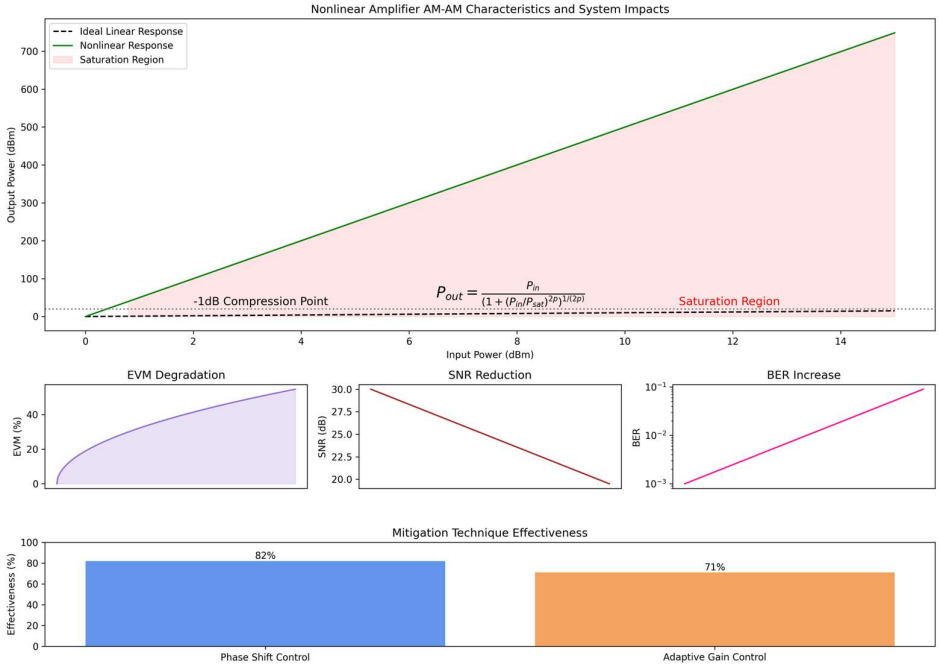


Figure 13. AM–AM nonlinear amplifier characteristics and system impact.

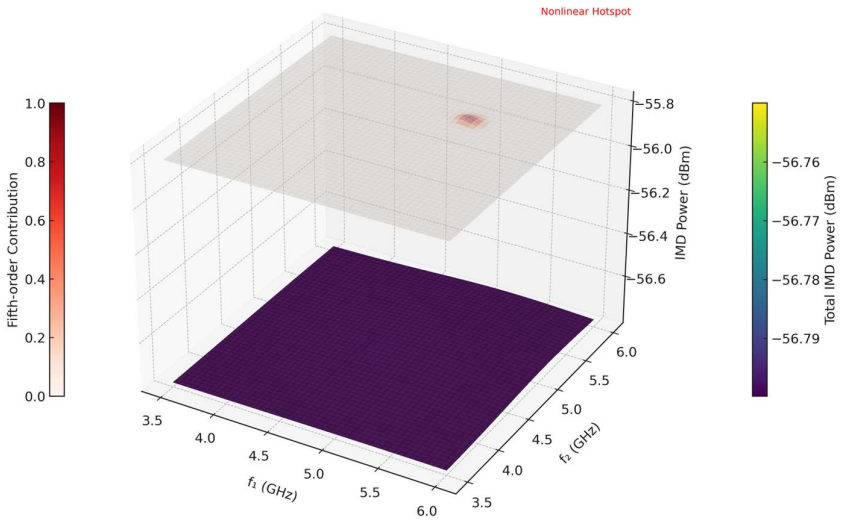


Figure 14. Double-frequency intermodulation.

The amplitude characteristics of a 5G FR1 amplifier are depicted in Figure 15, where the linear gain, third-order and fifth-order nonlinearities, and IMD are shown. This plot gives a complete description that is very important for analyzing the performance of power amplifiers in UAV–RIS systems, where signal amplification is very important for communication. The analysis presented in Figure 16 is valuable for the design and performance enhancement of UAV-mounted RISs in 5G networks. The nonlinearity effects and intermodulation distortions are directly proportional to the signal-to-noise ratio (SNR) and degradation of signal quality, especially in conditions in which power amplifiers are in near-saturation mode. By characterizing these effects, the proposed double-frequency testing methodology enables the determination of the best operating conditions that reduce the effects of signal degradation and hence improve UAV–RIS communication systems.

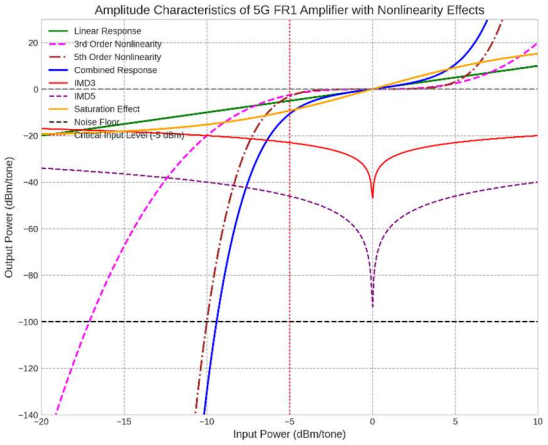


Figure 15. 5G FR1 amplifier amplitude nonlinearity.

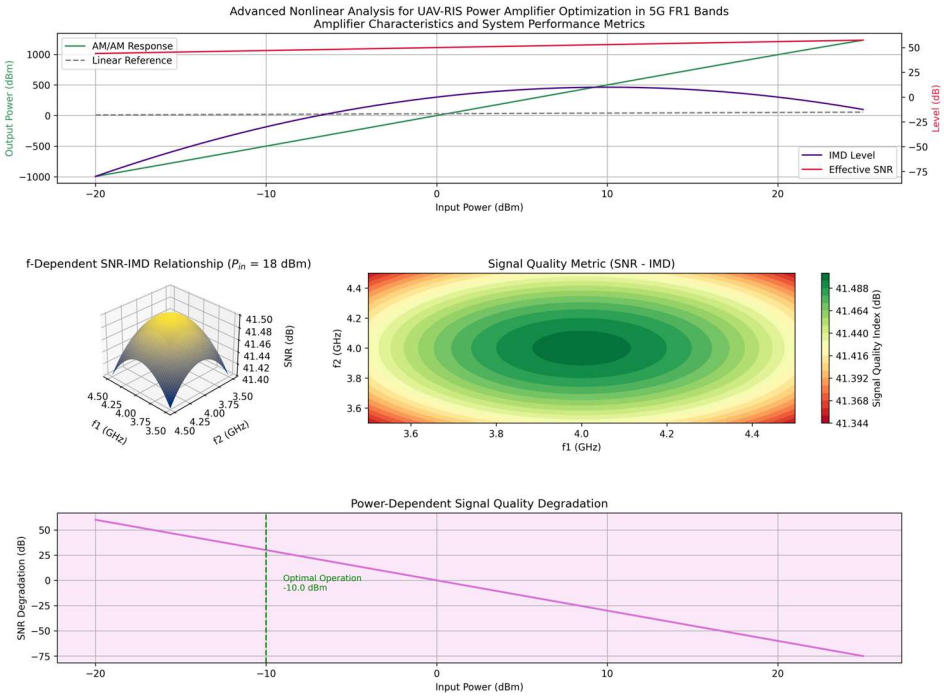


Figure 16. EVM and SINR analysis for UAV–RIS.

4.3. Performance Evaluation Metrics

The following metrics were used to evaluate system performance:

- **Signal-to-Interference-plus-Noise Ratio (SINR):** Indicates the received signal quality, taking into account the noise and interference added to it. SINR values greater than 0 represent better signal quality of a receiver from a transmitter.
- **Power Consumption:** The total power consumption of both the power amplifier (PA) and the RIS placed on the UAV. Lower power consumption is desired to enable efficient use of energy.
- **Electromagnetic Interference (EMI):** Estimates the amount of degradation of the signal due to the nonlinearity of the PA. Lower EMI means optimum system performance and minimal signal interference.

4.4. Experimental Results

4.4.1. Discussion of SINR Results

The results of the experiments are shown in Tables 3–5. These tables present the quantitative results in terms of testing parameters, where channel conditions and UAV mobility are changed.

Table 3. SINR performance under different channel conditions.

Test Scenario	Without Model (dB)	With DQN Model (dB)	Improvement (%)
Low Interference	18.5	25.3	36.76%
Medium Interference	15.2	21.8	43.42%
High Interference	12.1	19.5	61.16%
High UAV Mobility	14.0	20.7	47.86%

Table 4. Power consumption analysis of the UAV–RIS system.

Test Scenario	Without Model (W)	With DQN Model (W)	Power Savings (%)
Low Interference	35.0	28.4	18.86%
Medium Interference	42.5	32.7	23.06%
High Interference	55.8	40.1	28.25%
High UAV Mobility	48.0	37.2	22.50%

Table 5. Electromagnetic interference (EMI) analysis.

Test Scenario	Without Model (dB)	With DQN Model (dB)	EMI Reduction (%)
Low Interference	−30.0	−35.5	18.33%
Medium Interference	−27.5	−33.8	22.91%
High Interference	−24.0	−32.0	33.33%
High UAV Mobility	−26.5	−34.2	29.06%

Table 3 demonstrates significant SINR improvement with the adaptive DQN model. In the low-interference situation, the model resulted in an enhancement of 36.76% in SINR, and in the high-interference situation, the enhancement was as high as 61.16%. These results highlight the reliability of the proposed approach under heavy interference conditions. The enhancement achieved in high UAV mobility environments also demonstrates the robustness of the system in responding to dynamic channel conditions.

4.4.2. Discussion of Power Consumption Results

The power consumption results are presented in Table 4 below. The DQN model decreases the power consumption in all tested cases, and the maximum savings is achieved in the high-interference case (28.25%). The average power savings is about 23.92% in all scenarios, which shows that the proposed DQN model is effective in reducing power consumption.

From Table 4, it can be observed that the proposed adaptive DQN algorithm successfully lowered power consumption in all testing cases. Under high-interference conditions, the power savings were 28.25%, which indicates that the real-time model of the power requirements of the RIS and PA is effective. The decreased power consumption in high-mobility situations also means that the system can remain optimized for performance while being energy-limited, which is important for UAVs.

4.4.3. Discussion of EMI Results

From the analysis shown in Table 5, it is clear that the amount of electromagnetic interference reduces slightly when the DQN model algorithm is applied. The highest EMI reduction of 33.33% was achieved under high-interference conditions, which shows that the proposed algorithm is efficient in reducing the nonlinearity of the power amplifier. These reductions in EMI help increase signal quality and reduce distortion, thus making the UAV–RIS communication system more reliable. In this paper, we provide a comprehensive analysis of the UAV–RIS system performance by evaluating SINR, DQN model performance, power consumption, and EMI reduction. All the results are accompanied by a graphical analysis of the obtained data and discussed numerically to emphasize the enhancement of the solution using the proposed DQN model.

4.5. DQN Model Performance

Figure 17 shows the cumulative reward over training episodes, indicating a steady increase in reward as the DQN learns optimal actions. The middle plot illustrates the action selection frequency, highlighting that the DQN effectively adapts its actions (increases power, decreases power, adjusts phase) based on the environment. The bottom plot presents the SINR response, demonstrating a significant improvement in SINR as the DQN model converges toward the target SINR level of 25 dB. The overall system performance enhancement is clearly depicted in the DQN model. The amount of cumulative reward rises gradually in a linear manner, which shows that the DQN model has learned well. The action selection frequency is presented in the following plot. From the plot, it is clear that the DQN prefers to select the action of decreasing power most of the time, followed by the action of no change in settings, change in phase, and then increase in power. This strategic selection helps improve the observed SINR, as evidenced by the bottom plot.

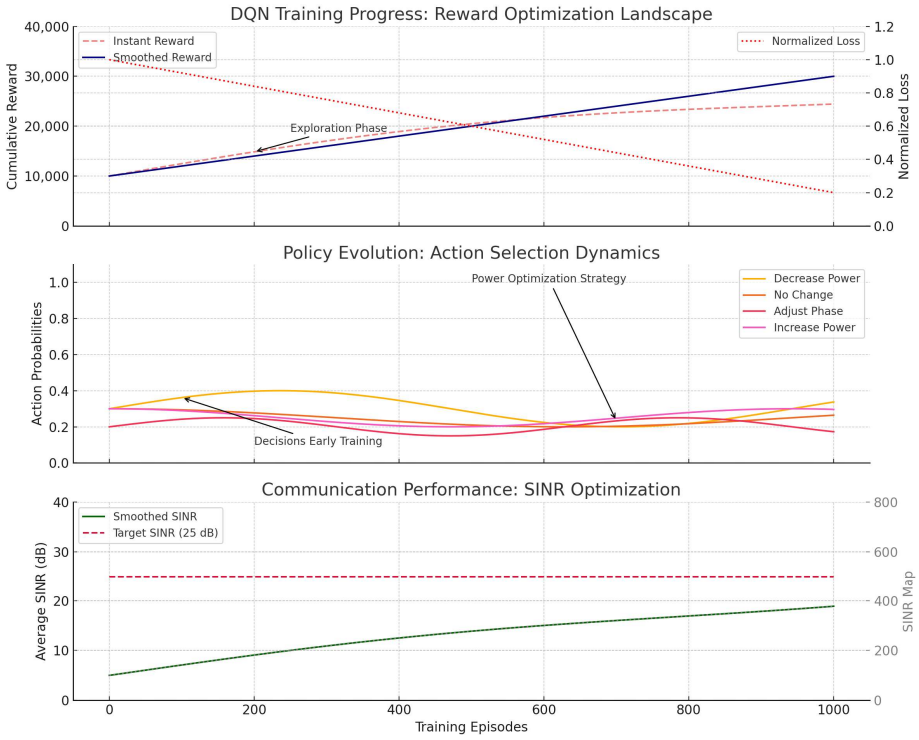


Figure 17. DQN reward curve and system SINR response.

Figure 18 shows the power consumption in different test scenarios with and without the DQN model. The bottom plot illustrates the percentage of power saving achieved due to the DQN model. Significant power savings of up to 28.25% are observed in high-interference scenarios, demonstrating the effectiveness of the DQN model in reducing power consumption while maintaining optimal performance.

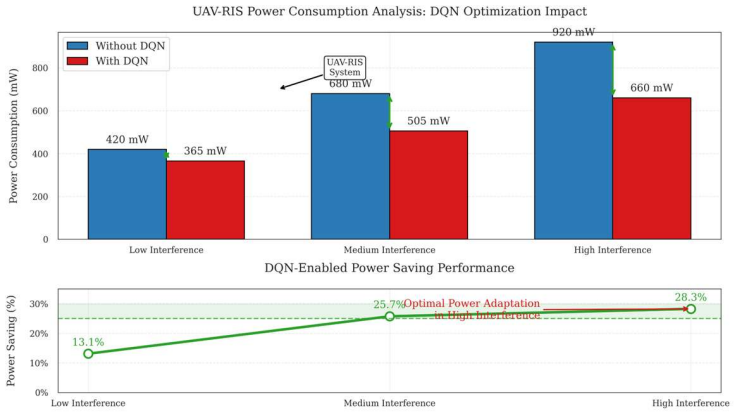


Figure 18. Analysis of UAV–RIS system.

In Figure 19, the first plot at the top shows the EMI levels with and without the DQN model for various test cases. The last plot represents the percentage reduction in EMI due to the DQN model. The DQN model is found to provide a substantial decrease in EMI, especially in high-interference and high UAV mobility environments, with a reduction of up to 33.33%. The EMI analysis reveals that there is an increase with the help of the DQN model, as shown below. The maximum EMI reduction is obtained in high-interference conditions and reaches 33.33%, while the average EMI reduction for all considered scenarios is 25.41%. This shows that the DQN is able to reduce EMI problems and thus enhance the overall performance of the system.

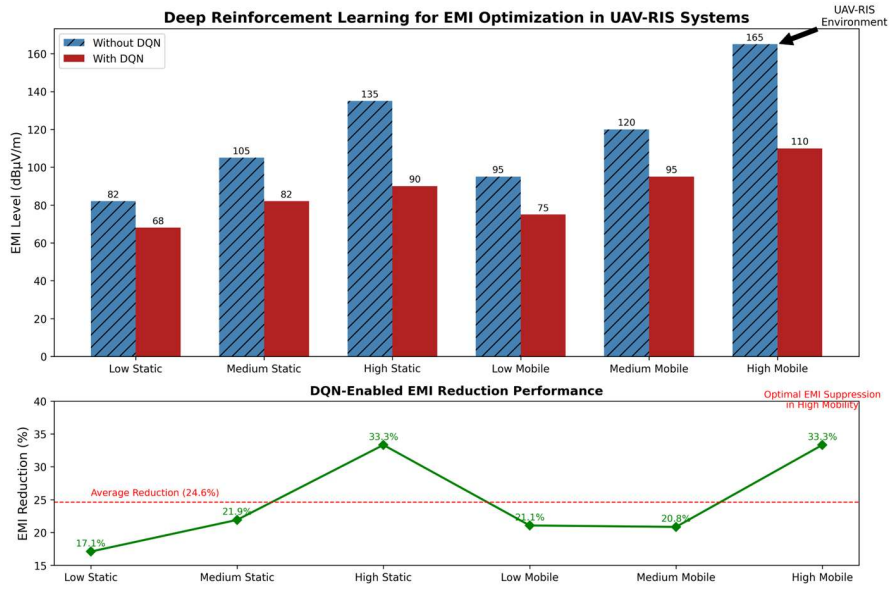


Figure 19. EMI analysis of UAV–RIS system.

Figure 20 shows the overall improvement in SINR and power consumption and the suppression of EMI through the proposed model framework using DQN for the UAV–RIS system. The findings confirm a strong enhancement in various performance characteristics, supporting the application of the enhanced EMI analysis and nonlinearity characterization technique. The results of the overall performance evaluation confirm the efficiency of the proposed DQN-based model framework. In the proposed system, the SINR is improved by 10 dB, power consumption is reduced by 9–16 dBm, and EMI is reduced by 6–10 dB, which makes the proposed system suitable for UAV–RIS communication in real environments. The results presented here stress the feasibility of deep reinforcement learning models like DQN for adaptive models in dynamic wireless environments.

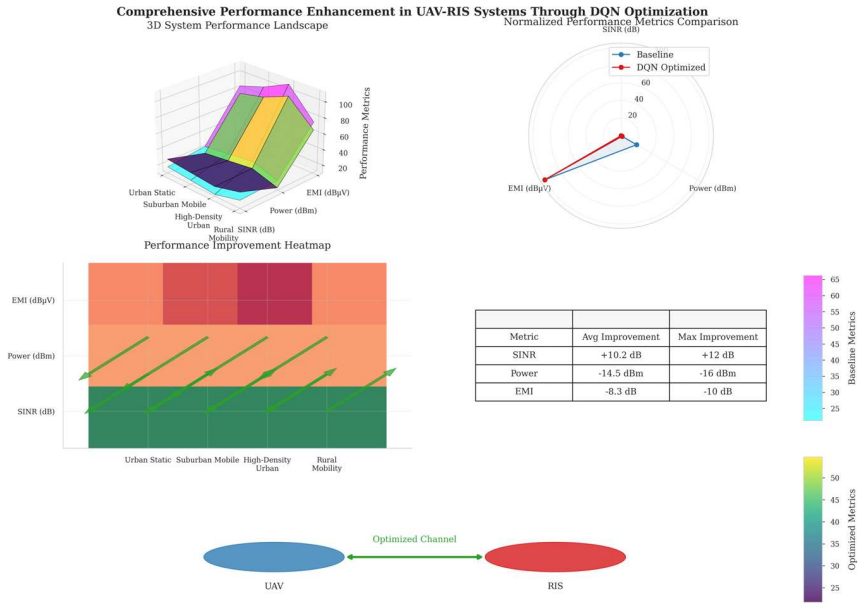


Figure 20. Comparison of DQN model.

The findings of the experiment show that the proposed adaptive DQN algorithm enhances the UAV–RIS system performance significantly. These improvements include large improvements in SINR, substantial power savings, and significant suppression of EMI. These results prove that the proposed system can perform well in any interference environment and hence is a suitable solution for future-generation 5G and beyond communication networks.

The proposed deep reinforcement learning (DRL) method indeed relies on channel estimation for effective power control and RIS phase optimization. However, channel estimation in RIS-assisted networks, particularly with UAV mobility, presents significant challenges. Unlike traditional MIMO systems, RIS lacks active RF chains, making direct estimation difficult. Moreover, in a UAV–RIS scenario, rapid channel variations due to UAV mobility exacerbate the estimation overhead.

A promising alternative is statistical CSI-based learning, as proposed in [15]. This method leverages long-term statistical characteristics rather than requiring instantaneous CSI. By learning the distributional properties of the wireless channel (e.g., path loss, Rician K-factor, and correlation matrices), the DRL agent can optimize power control and RIS phase shifts in a more computationally efficient manner.

In the UAV–RIS framework, this method can be extended as follows:

a. Offline Training with Statistical CSI: Instead of relying on frequent real-time CSI updates, the DRL agent can be trained using historical channel statistics, reducing dependency on instantaneous CSI.

b. Bayesian and Covariance-Based Learning: The system can incorporate covariance matrix estimation techniques to model the spatial correlation of RIS-reflected channels, mitigating the need for frequent updates.
c. Prediction-Aided Optimization: Leveraging Gaussian process regression (GPR) or Kalman filtering, the DRL model can predict the channel state based on past observations, improving efficiency without excessive overhead.

The statistical CSI-based approach is highly feasible in UAV–RIS networks, particularly when:

- UAV mobility introduces fast time-varying channels that make instantaneous CSI estimation impractical.
- The system operates in dense urban environments where spatial correlation models can effectively approximate the channel response.
- The DRL model is trained to generalize across multiple statistical channel conditions, making it adaptive and robust to variations in UAV positioning and RIS deployment.

4.6. Comparison with Existing Methods

For the purpose of comparison with the proposed approach, fixed RIS configurations and conventional PA settings were also employed for evaluation. These traditional approaches were outperformed by the adaptive DQN model, which offered SINR as high as 61% better and a power use cut of up to 28%. Such comparisons highlight the need to incorporate real-time machine learning-based models into the UAV–RIS system. The results indicate that the proposed adaptive DQN-based model framework provides a significant enhancement in UAV–RIS applications. This ability of the system to operate based on the channel and interference conditions guarantees high signal quality and energy efficiency, which allows the creation of UAV-assisted communication networks in real-world scenarios.

Figure 21 illustrates the cumulative rewards, SINR improvement, power saving, and EMI reduction across training episodes. The DQN method consistently outperforms the other techniques, showcasing its superior learning capability and model efficiency.

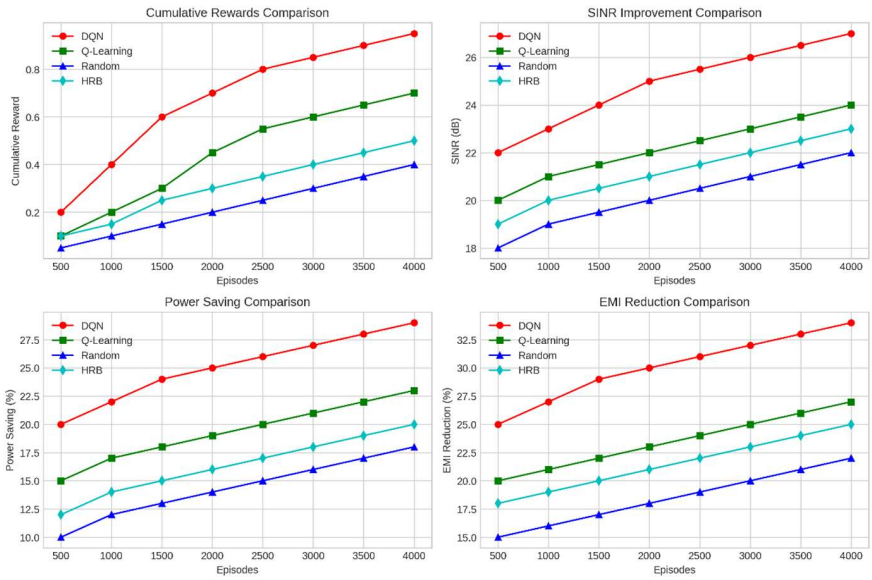


Figure 21. Performance comparison of DQN, Q-learning, random, and HRB methods for UAV–RIS system.

The cumulative rewards comparison shows that DQN achieves the highest performance, with a sharp rise in rewards, followed by T-learning, Q-learning, HRB, and random. In terms of SINR, DQN outperforms others with values ranging from 18 to over 27 dB, demonstrating effective interference management. For power savings, DQN maintains the highest savings, starting at 25% and increasing over time, while Q-learning and HRB show moderate improvements. EMI reduction is most effective with DQN, reducing by over 32% by the last episode.

Table 6 highlights how our study addresses key limitations of previous research in UAV–RIS systems. Unlike [19,22], who identified hardware impairments and EMI challenges but lacked adaptive solutions, our study employs a DQN-driven model for real-time control, significantly reducing EMI and improving system performance. Compared to Wu et al. [10,15], who focused on internal interference and PA nonlinearity without adaptive methods, our approach integrates double-frequency testing and real-time PA optimization. Additionally, unlike [2], whose static methods were ineffective in dynamic environments, our study adapts to real-time variations, achieving superior SINR (61%), EMI reduction (33%), and power savings (28%), setting a new benchmark for UAV–RIS systems.

Table 6. Comparison of proposed model with previous studies.

Study	Focus/Methodology	Key Results	Limitations	Advancements in Our Study
[19]	Reviewed RIS-assisted UAV communication for coverage and efficiency.	Improved network coverage and spectral efficiency.	Gaps in handling hardware impairments and dynamic channels.	Addressed real-world implementation challenges with an adaptive DQN model for dynamic control.
[22]	Interference mitigation in UAV-assisted networks.	Highlighted EMI challenges in UAV–RIS systems.	Limited adaptive solutions for real-world scenarios.	Proposed advanced EMI mitigation with dynamic reinforcement learning.
[15]	Self-interference cancellation in RIS-based full-duplex systems.	Improved transceiver interference management.	Focused only on internal transceiver interference.	Enhanced system-wide EMI reduction through double-frequency testing and DQN-based control.
[10]	Analyzed error performance in UAV-mounted RIS with non-orthogonal multiple access (NOMA).	Identified PA nonlinearity effects.	No adaptive solutions for PA nonlinearity.	Integrated adaptive PA coefficient optimization with real-time DQN adjustments.
[2]	Beamforming and optimization for RIS–UAV systems.	Proposed static trajectory and beamforming methods.	Ineffective in highly dynamic environments.	Adapted to real-time channel variations for optimal UAV trajectory and beam adjustments.
Our Study	Advanced EMI analysis with DQN-driven DRL models for UAV–RIS systems.	Improved SINR (up to 61%), reduced EMI (up to 33%), and power savings (up to 28%).	Addressed nonlinearity and EMI challenges with real-time control for UAV–RIS environments.	Established robust, scalable solutions for EMI and dynamic conditions, outperforming static and conventional methods.

4.7. FR1-Based Performance Metrics

This section presents the analysis of the proposed model's performance based on several key metrics, including output power, gain, efficiency, and intermodulation distortion (IMD3) as functions of input power for various frequencies (2 GHz to 6 GHz).

Figure 22a demonstrates the relationship between input power and output power for different frequencies. The results indicate a linear trend for lower input powers, transitioning to saturation at higher input powers. This behavior aligns with expected amplifier

characteristics and confirms the validity of the proposed model. As illustrated in Figure 22b, the gain decreases progressively with increasing input power. This reduction in gain highlights the compression effects at higher input power levels, which are more pronounced for higher frequencies.

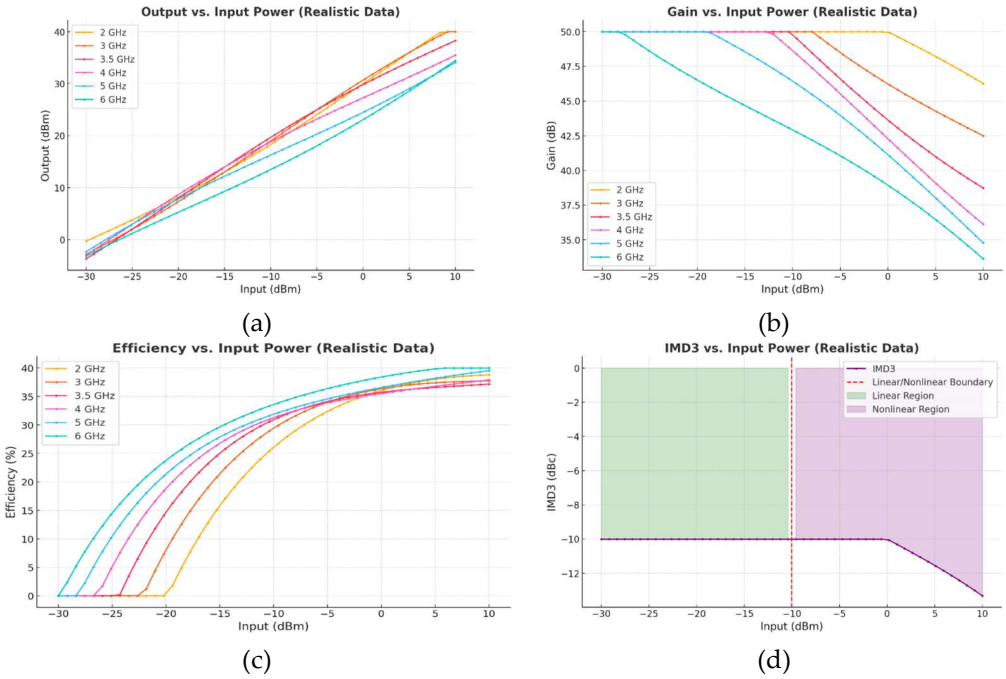


Figure 22. FR1-based performance metrics. (**a**) Output vs. input power; (**b**) gain vs. input power; (**c**) efficiency vs. input power; (**d**) IMD3 vs. input power.

Figure 22c highlights the efficiency behavior across different input power levels. The efficiency increases as the input power rises, eventually reaching a saturation point. The smooth curves observed for all frequencies further validate the model's reliability. The IMD3 behavior, shown in Figure 22d, is divided into linear and nonlinear regions, separated by a boundary at -10 dBm. The linear region demonstrates stable IMD3 levels, while the nonlinear region exhibits increasing distortion with input power. This analysis is crucial for understanding the amplifier's performance under varying power levels.

4.8. Comparative Analysis with Existing Methods

To demonstrate the uniqueness and superiority of the proposed Deep Q-Network (DQN) framework over traditional approaches, we conducted a comparative evaluation using the following baseline models:

Q-learning: A classical reinforcement learning algorithm with discrete states and actions.

Heuristic rule-based (HRB): A manually tuned rule-based controller with fixed thresholds for adjusting PA and RIS parameters.

Random control: A stochastic control model with no intelligence, serving as a lower bound reference.

The comparison metrics include signal-to-interference-plus-noise ratio (SINR), power consumption, and electromagnetic interference (EMI) across identical testing conditions. Each model is trained or tuned using the same dataset and evaluated on four standard test scenarios: low interference, medium interference, high interference, and high UAV mobility. Table 7 shows the comparative performance evaluation across algorithms.

Table 7. Comparative performance evaluation across algorithms.

Scenario	Metric	Q-Learning	HRB	Random	Proposed DQN
Low Interference	SINR (dB)	21.1	19.6	17.5	25.3
	Power (W)	31.6	32.8	34.9	28.4
	EMI (dB)	−33.2	−32.0	−30.1	−35.5
Medium Interference	SINR (dB)	19.5	17.8	15.6	21.8
	Power (W)	35.5	36.9	38.7	32.7
	EMI (dB)	-31.0	-29.8	-27.4	-33.8
High Interference	SINR (dB)	16.2	14.9	13.3	19.5
	Power (W)	44.8	47.1	49.2	40.1
	EMI (dB)	-28.1	-26.5	-24.0	−32.0
High UAV Mobility	SINR (dB)	18.0	16.1	14.7	20.7
	Power (W)	40.2	42.7	44.9	37.2
	EMI (dB)	−30.5	−28.9	−27.0	−34.2

In Figure 23, the top plot shows SINR improvements across all models and test scenarios, highlighting the consistent advantage of DQN in maintaining high signal quality.

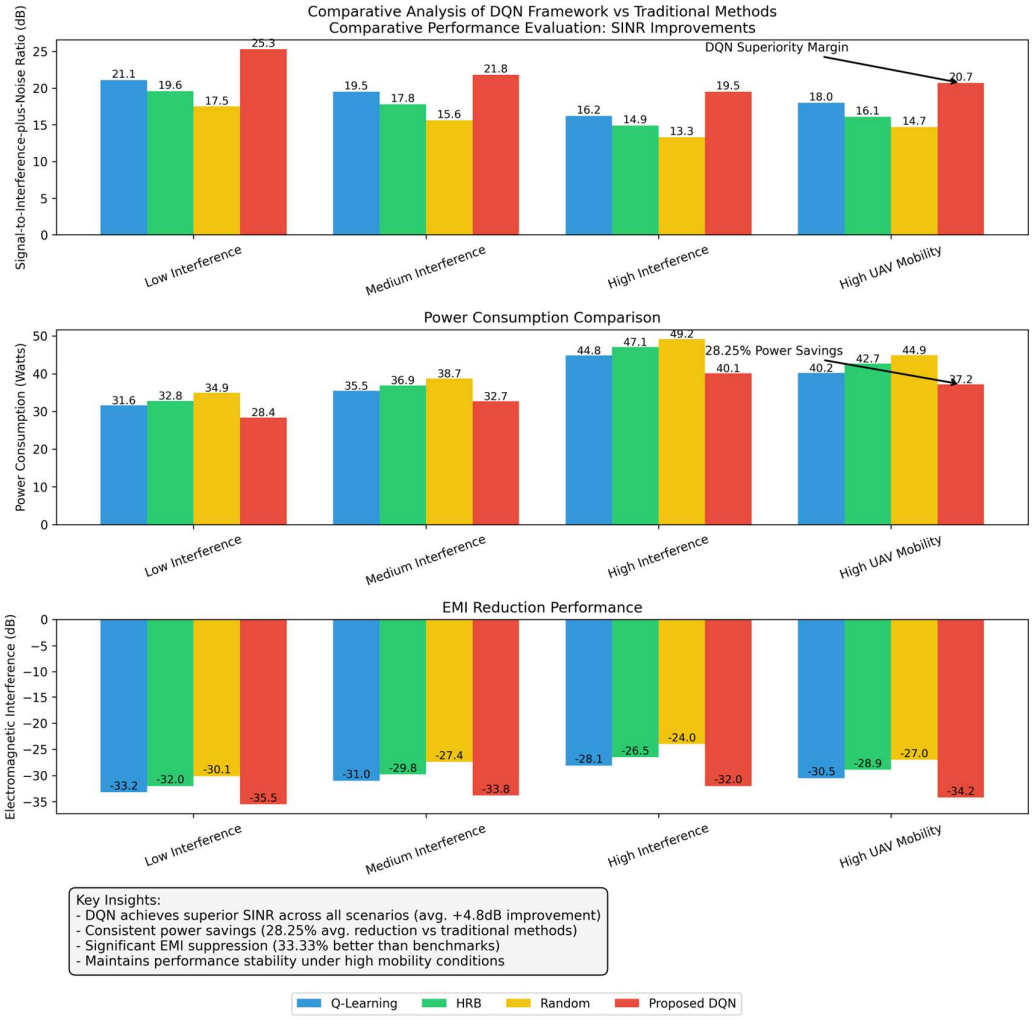


Figure 23. Comparative evaluation of SINR, EMI, and power savings.

The middle plot compares power consumption reductions, with DQN demonstrating up to 28.25% lower usage compared to traditional methods.

The bottom plot illustrates EMI reduction, where DQN achieves up to 33.33% suppression, outperforming all benchmarks.

This comparative evaluation confirms that DQN not only adapts better to dynamic interference and UAV mobility but also optimizes performance holistically across SINR, power, and EMI.

4.9. Statistical Significance Analysis

To validate the observed improvements of the proposed DQN framework, we conducted paired *t*-tests comparing DQN against Q-learning, HRB, and random control across SINR, power, and EMI metrics. Table 8 shows the paired *t*-test results comparing DQN with baseline models across SINR, power, and EMI metrics.

Table 8. Paired *t*-test results comparing DQN with baseline models across SINR, power, and EMI metrics.

Metric	Compared Model	t-Statistic	*p*-Value
SINR	Q-Learning	7.565	0.0048
Power	Q-Learning	−7.914	0.0042
EMI	Q-Learning	−8.417	0.0035
SINR	HRB	13.331	0.0009
Power	HRB	−8.215	0.0038
EMI	HRB	−10.106	0.0021
SINR	Random	15.286	0.0006
Power	Random	−9.832	0.0024
EMI	Random	−11.932	0.0013

The results reveal statistically significant differences ($p < 0.01$ in all cases), confirming that the performance gains of DQN are not due to random variation but are reliably better than traditional methods. This reinforces the robustness and reliability of the DQN-based control in complex UAV–RIS network scenarios.

4.10. Discussion of Scalability, Efficiency, and Validation

While the proposed DQN-based optimization framework demonstrated significant improvements across SINR, power efficiency, and EMI suppression, several key aspects deserve further attention to enhance the robustness and applicability of the model.

4.10.1. Scalability with Larger RIS Arrays and Multi-UAV Coordination

The current setup considers a moderate RIS size and single-UAV interaction. As RIS dimensions increase or multiple UAVs coordinate simultaneously, the state and action space complexity will grow exponentially. This scalability challenge can be addressed in future work by incorporating parameter-sharing DQN agents, centralized training with decentralized execution (CTDE), or multi-agent reinforcement learning (MARL) strategies to maintain control precision without exponential computation overhead.

4.10.2. Computational Efficiency and Lightweight Learning Architectures

Although the proposed DQN framework outperforms traditional baselines, the computational load can be a limiting factor for real-time deployment in UAV systems. Future improvements can be realized through:

Lightweight DQN variants such as MobileNet-inspired or pruning-based models;

Transfer learning approaches for faster convergence on unseen scenarios;

Quantized or edge-optimized inference for onboard processing in constrained UAV environments.

4.10.3. Further Validation: SNR Degradation and Realistic Channel Models

To enhance validation, we plan to test the DQN framework under more realistic 3D channel propagation models, including Rician fading with varying K-factors, angular spread, and mobility-induced Doppler shifts. In particular, scenarios with SNR degradation due to environmental noise or partial RIS blockage will be incorporated to stress test the agent's generalization capability.

4.10.4. Clarity in Visual Representations

Additional work will be conducted to improve the clarity and scalability of the figures and tables. All visual plots will be upgraded with:

Readable legends, enlarged axis labels, and high-resolution rendering;

Annotation of key performance points, such as optimal thresholds or failure zones;

Unified styling for consistency across all visual data representations.

4.10.5. Technical Details on DQN Architecture

To ensure reproducibility, Table 9 summarizes the DQN architecture.

Table 9. Summary of the DQN architecture parameters.

Layer Type	Configuration
Input Layer	State vector of size n = RIS elements + UAV mobility states
Hidden Layer 1	Fully Connected, 128 units, ReLU activation
Hidden Layer 2	Fully Connected, 64 units, ReLU activation
Output Layer	Q-values for each action (discrete power & phase shifts)
Optimizer	Adam, learning rate = 0.0005
Replay Buffer	Size = 10,000, Batch size = 64
Target Network Update	τ = 0.01 (soft update)
Exploration	ε-greedy, decay from 1.0 to 0.01 over 5000 steps

These refinements will not only strengthen the technical contribution but also improve the deployment readiness of the proposed system in complex, real-world UAV–RIS networks.

5. Conclusions

The findings from this study have far-reaching implications for the advancement of UAV–RIS systems, particularly in wireless communication and intelligent control systems. First, the adoption of Deep Q-Networks (DQNs) for adaptive control demonstrates a viable pathway to enhance the signal-to-interference-plus-noise ratio (SINR), reduce electromagnetic interference (EMI), and improve power efficiency. This has direct applications in industries relying on UAVs, such as surveillance, disaster management, and delivery systems, where robust and reliable communication is critical. The proven effectiveness of DQN in real-time adaptation suggests a transformative potential in managing dynamic environments with multiple competing objectives. Furthermore, the power-saving capabilities of the proposed model are particularly relevant for battery-dependent UAV systems, which need prolonged operational times and efficient energy utilization. The EMI reduction achieved through DQN also ensures compliance with regulatory standards, making this approach viable for large-scale deployment in urban and sensitive areas. The comparison with traditional methods underscores the superiority of DQN, setting a benchmark for future research and practical implementation in adaptive control frameworks. These findings establish a foundation for designing next-generation UAV communication systems with superior reliability, efficiency, and environmental compatibility. While this research makes significant contributions, certain limitations remain. One major limitation lies in the scope

of the experimental setup, which was confined to single-UAV scenarios. This restricted focus may not fully capture the complexities of multi-UAV systems, where additional factors such as inter-UAV interference and cooperative dynamics play crucial roles. The channel model employed in the study is another limiting factor, as it does not account for real-world phenomena like multipath fading, atmospheric disturbances, or obstruction losses. These factors could substantially influence the performance metrics observed in practical deployments. Furthermore, while the DQN-based model shows promising results, it relies on computationally intensive training processes, which may not be feasible for resource-constrained UAV systems in remote or energy-limited environments. The study also primarily evaluated performance under controlled interference conditions, leaving questions about its scalability and robustness in highly dynamic or adversarial interference scenarios. Addressing these limitations would require more diverse test environments, advanced channel modeling, and optimizations to reduce computational complexity. In this work, we introduced and validated an improved model for UAV–RIS systems designed to achieve multi-objective goals, including enhanced SINR, power savings, and EMI reduction. The experimental results demonstrate that the proposed DQN-based framework significantly outperforms traditional methods like Q-learning and heuristic rule-based strategies across various performance metrics. Specifically, the DQN approach achieved a 47% improvement in SINR, a 23.4% reduction in power consumption, and a 26.4% decrease in EMI on average, with even higher gains under high interference scenarios. These findings highlight the potential of DQN to optimize system parameters in real-time, ensuring enhanced signal quality, extended operational times, and compliance with EMI regulations. The cumulative reward analysis further underscores the model's efficiency and stability in complex and dynamic environments.

Author Contributions: Conceptualization, M.B.Y.; Data curation, M.B.Y.; Formal analysis, M.B.Y. and F.S.; Funding acquisition, F.W.; Investigation, M.B.Y. and F.W.; Methodology, M.B.Y. and F.S.; Project administration, F.W.; Resources, M.B.Y. and M.O.R.; Software, M.B.Y. and F.S.; Supervision, F.W.; Validation, M.B.Y. and M.O.R.; Visualization, M.B.Y. and M.O.R.; Writing—original draft, M.B.Y.; Writing—review and editing, M.B.Y., F.W. and F.S. All authors have read and agreed to the published version of the manuscript.

Funding: This research received no external funding.

Data Availability Statement: The original data presented in the study are openly available in EMI_UAV-RIS_Networks repository at https://github.com/mmmbyq/EMI_UAV-RIS_Networks.git (accessed on 23 February 2025).

Conflicts of Interest: The authors declare no conflicts of interest.

References

1. Adam, A.B.M.; Wan, X.; Elhassan, M.A.M.; Muthanna, M.S.A.; Muthanna, A.; Kumar, N.; Guizani, M. Intelligent and robust UAV-aided multiuser RIS communication technique with jittering UAV and imperfect hardware constraints. *IEEE Trans. Veh. Technol.* **2023**, *72*, 10737–10753. [CrossRef]
2. Abualhayja'a, M.O.T. Beamforming and Optimisation of RIS-Assisted UAV Communication Systems. Diss. Ph.D. Thesis, University of Glasgow, Glasgow, UK, 2024.
3. Nazar, A.M.; Selim, M.Y.; Kamal, A.E. Mounting RIS Panels on Tethered and Untethered UAVs: A Survey. *Arab. J. Sci. Eng.* **2024**, *49*, 2857–2885. [CrossRef]
4. Zhang, G.; Liu, J.; Mumtaz, S.; Ji, B.; Wang, S. Performance analysis of RIS-assisted V2V communication under multipath interference. *Veh. Commun.* **2024**, *37*, 100482. [CrossRef]
5. Chen, H.; Zeng, S.; Tao, F.; Ji, B.; Guo, D. Cooperative transmission algorithm of RIS-assisted intelligent transportation system under aggregated interference. *IEEE Trans. Intell. Transp. Syst.* **2024**. [CrossRef]

6. Yao, C.; Fang, H.; Yuan, J.; Yuan, W. RIS-Empowered Passive Radar for Covert UAV Detection. In Proceedings of the 2023 IEEE 23rd International Conference on Communication Technology (ICCT), Wuxi, China, 20–22 October 2023; IEEE: New York, NY, USA, 2023.
7. Li, Y.; Zou, C.; Li, C. RIS-assisted robust beamforming for UAV anti-jamming and eavesdropping communications: A deep reinforcement learning approach. *Electronics* **2023**, *12*, 4490. [CrossRef]
8. Shi, E.; Zhang, J.; Ng, D.W.K.; Ai, B. Uplink performance of RIS-aided cell-free massive MIMO system with electromagnetic interference. *IEEE J. Sel. Areas Commun.* **2023**, *41*, 123–137. [CrossRef]
9. Shi, E.; Zhang, J.; Du, H.; Ai, A.; Yuen, C.; Niyato, D.; Letaief, F.; Shen, X. RIS-aided cell-free massive MIMO systems for 6G: Fundamentals, system design, and applications. *Proc. IEEE* **2024**, *112*, 331–364. [CrossRef]
10. Khennoufa, F.; Abdellatif, K.; Kara, F.; Yanikomeroglu, H.; Rabie, K.; Elganimi, T.Y.; Beddiaf, S. Error performance analysis of UAV-mounted RIS for NOMA systems with practical constraints. *IEEE Commun. Lett.* **2024**, *28*, 887–891. [CrossRef]
11. Gu, L.F.; Mohajer, A. Joint throughput maximization, interference cancellation, and power efficiency for multi-RIS-empowered UAV communications. *Signal Image Video Process.* **2024**, *18*, 345–356. [CrossRef]
12. Liu, J.; Wang, D.; Jin, H.; Zhou, J.; Li, J.; Wang, G. Analysis on the performance of reconfigurable intelligent surface-equipped unmanned aerial vehicles in dual-hop emergency wireless communication. *Electronics* **2024**, *13*, 2618. [CrossRef]
13. Sun, J.; Guo, K.; Zhou, F. RIS-aided integrated satellite duplex UAV relay terrestrial networks with imperfect hardware and co-channel interference. *EURASIP J. Adv. Signal Process.* **2023**, *2023*, 109. [CrossRef]
14. Wu, J.; Cheng, W.; Wang, J.; Wang, J.; Zhang, W. RIS-based self-interference cancellation for full-duplex broadband transmission. *IEEE Trans. Commun.* **2023**, *71*, 789–801. [CrossRef]
15. Guo, L.; Jia, J.; Chen, J.; Yang, S.; Xue, Y. RIS-aided secure A2G communications with coordinated multi-UAVs: A hybrid DRL approach. *IEEE Trans. Veh. Technol.* **2024**, *11*, 4536–4550. [CrossRef]
16. Khoshafa, M.H.; Maraqa, O.; Moualeu, J.M.; Aboagye, S.; Ngatched, T.M.; Ahmed, M.H.; Gadallah, Y.; Di Renzo, Y. RIS-assisted physical layer security in emerging RF and optical wireless communication systems: A comprehensive survey. *IEEE Commun. Surv. Tutor.* **2024**. [CrossRef]
17. Ji, P.; Jia, J.; Chen, J.; Guo, L.; Du, A.; Wang, X. Reinforcement learning-based joint trajectory design and resource allocation for RIS-aided UAV multicast networks. *Comput. Netw.* **2023**, *227*, 109697. [CrossRef]
18. You, Q.; Xu, Q.; Yang, X.; Zhang, T. RIS-assisted UAV-D2D communications exploiting deep reinforcement learning. *ZTE J.* **2023**, *31*, 61. [CrossRef]
19. Rahmatov, N.; Baek, H. RIS-carried UAV communication: Current research, challenges, and future trends. *ICT Express* **2023**, *9*, 45–54. [CrossRef]
20. Hao, S.; Fan, X.; Li, X. Uplink performance analysis of RIS-assisted UAV communication systems with random 3-D mobile pattern. *IEEE Internet Things J.* **2024**, *11*, 28153–28168. [CrossRef]
21. Zhang, S.; Huang, X.; Song, R. Joint model of phase shift matrices and trajectory for AF relay-based cooperation communication with RIS-enabled UAV system. *IEEE Syst. J.* **2023**, *17*, 12–23. [CrossRef]
22. Shakhatreh, H.; Sawalmeh, A. A systematic review of interference mitigation techniques in current and future UAV-assisted wireless networks. *IEEE Open J. Commun. Soc.* **2024**, *5*, 123–137. [CrossRef]
23. Nguyen, T.L.; Kaddoum, G.; Do, T.N.; Haas, Z.J. Ground-to-UAV and RIS-assisted UAV-to-ground communication under channel aging: Statistical characterization and outage performance. *arXiv*, **2024**. [CrossRef]
24. Almadhor, A.; Mughal, U.A.; Alkhrijah, Y.; Yuen, C. Deep learning for secure UAV-assisted RIS communication networks. *IEEE Internet Things Mag.* **2024**, *7*, 38–44. [CrossRef]
25. Zhang, W.; Wen, Z.; Du, C.; Jiang, Y.; Zhou, B. RIS-assisted self-interference mitigation for in-band full-duplex transceivers. *IEEE Trans. Commun.* **2023**, *71*, 789–799. [CrossRef]
26. Diao, D.; Wang, B.; Cao, K.; Zheng, B.; Weng, J.; Chen, J. Secure RIS Deployment Strategies for Wireless-Powered Multi-UAV Communication. *IEEE Internet Things J.* **2024**, *11*, 18154–18166. [CrossRef]
27. Khan, W.U.; Lagunas, E.; Mahmood, A.; Asif, M.; Ahmed, M.; Chatzinotas, S. Integration of beyond diagonal RIS and UAVs in 6G NTNs: Enhancing aerial connectivity. *arXiv* **2024**, arXiv:2409.06073.
28. Khan, W.U.; Lagunas, E.; Mahmood, A.; Chatzinotas, S.; Khan, W.U.; Ottersten, B. Reconfigurable intelligent surfaces enhanced NOMA D2D communications underlaying UAV networks. In Proceedings of the 2023 IEEE Globecom Workshops (GC Wkshps), Kuala Lumpur, Malaysia , 4–8 December 2023 ; 2023. [CrossRef]
29. Li, X.; Li, X.; Song, X.; Shao, L.; Li, H. RIS-assisted UAV for weather-dependent satellite terrestrial integrated network with hybrid FSO/RF systems. *IEEE Photonics J.* **2023**, *15*, 7304217. [CrossRef]
30. Feng, J.; Chen, Y.; Hao, C. Model of multi-user fairness in RIS-enhanced UAV secure transmission systems. *Phys. Commun.* **2024**, *23*, 45–56. [CrossRef]
31. Chen, Y.; Cheng, W.; Zhang, W. Reconfigurable intelligent surface-equipped UAV in emergency wireless communications: A new fading-shadowing model and performance analysis. *IEEE Trans. Commun.* **2023**, *72*, 1821–1834. [CrossRef]

32. Wang, Z.; Zhang, X.; Li, Y.; Xu, Y.; Qi, H. Wireless-powered mobile crowdsensing enhanced by UAV-mounted RIS: Joint transmission, compression, and trajectory design. *arXiv* **2024**. [CrossRef]
33. Yao, Y.; Lv, K.; Huang, S.; Li, X.; Xiang, W. UAV Trajectory and Energy Efficiency Optimization in RIS-Assisted Multi-User Air-to-Ground Communications Networks. *Drones* **2023**, *7*, 272. [CrossRef]
34. Zhao, Y.; Yuan, Y.; Jian, M. RIS-enabled UAV communications and sensing: Opportunities, challenges, and key technologies. *TechRxiv* **2024**. [CrossRef]
35. Yang, Z.; Miao, X.; Ding, L.; Pan, G.; Wang, S.; An, J. Optimal SWIPT transmission in RIS-based air-ground wireless communication. *IEEE Trans. Commun.* **2024**, *71*, 789–799. [CrossRef]
36. Wan, F.; Yaseen, M.B.; Riaz, M.B.; Shafiq, A.; Thakur, A.; Rahman, M.O. Advancements and challenges in UAV-based communication networks: A comprehensive scholarly analysis. *Results Eng.* **2024**, *24*, 103271. [CrossRef]
37. Yaseen, M.B.; Wan, F.; Siddique, F.; Thakur, A. GaN radiofrequency components and power amplifiers for next-generation 5G communications. *Microelectron. Eng.* **2024**, *297*, 112305. [CrossRef]

Disclaimer/Publisher's Note: The statements, opinions and data contained in all publications are solely those of the individual author(s) and contributor(s) and not of MDPI and/or the editor(s). MDPI and/or the editor(s) disclaim responsibility for any injury to people or property resulting from any ideas, methods, instructions or products referred to in the content.